Master Thesis

submitted within the UNIGIS MSc programme
Department of Geoinformatics
University of Salzburg

Geomorphologic Analysis of the Mondsee Catchment

by

MSc. Sofia Koroxenidou
106697, UNIGIS MSc Year of 2020

A thesis submitted in partial fulfilment of the requirements of the degree of
Master of Science – MSc

Advisor:

Hermann Klug

Konstanz, 23.10.2022

Contents

Abstract

In recent decades advances in Geographical Information Systems (GIS) have extensively contributed to Geosciences. Geomorphology is a discipline that benefited from these advances as it is associated with land-surface, and spatiotemporal analysis, the focal point of GIS. This work emphasizes the importance of GIS in geomorphological analyses and aims to digitize written scientific knowledge, while demonstrating the extent of its contribution to the process. The Catchment area of Lake Mondsee, in Austria was chosen as a study site due to its relevance to the Alpine glaciers and the characteristic landforms that they left behind while receding. A DEM derived from LiDAR data in combination with ESRI's ArcGIS Pro toolboxes was used for the analysis. Images found in literature were Georectified and used for ice reconstruction. Sightings of landforms were translated into point features and interpolated. Object- and Pixel-based image analyses were used on geological maps to extract a geomorphological map. The results, which were also summarized in a Story Map, demonstrate the extent and importance of GIS in geomorphological analysis as well as its versatility. They reveal that it can be also used in the field in combination with other web applications presenting a holistic spatial view of the area, while at the same time helping with the analysis.

1 Introduction

Geomorphology is the discipline that studies the genesis and evolution of landforms created by diverse processes on the Earth's surface and has applications in many fields, such as geology, geography, geodesy, etc. Glacial Geomorphology, as a subdiscipline, focuses on landforms shaped by glaciers a thousand years ago as a result of their movement, and erosive nature. It has a primary goal to "provide physically-based explanations of past, present, and future impacts of glaciers and ice sheets on landform and landscape development" (Harbor 1993).

Both Geomorphology and Glacial Geomorphology are associated with land-surface analysis and spatiotemporal analysis, extending the first law of geography where "*everything is related to everything else, but near things are more related than distant things*" (Tobler 1970). They attempt to characterize, and categorize the various landforms, as well as contribute to the why and how they are formed. The most essential tool used for the representation of the landforms in relation to their spatial reference is geomorphological mapping, the product of geomorphological analysis.

For the past two centuries, the methodology of the analysis has had two key elements at its core: field work and thematic mapping. Through field surveys the knowledge gained from mapping features is transferred to topographic maps of various scales, small 1:10.000 and large 1:5.000. Thematic mapping is an extension of field mapping associated with specific scientific questions, such as the ice mass, ice height, or glacial landforms (Demek 1972; Leser and Stäblein 1975; Robinson et al. 1995; Gustavsson et al. 2006). The resulting maps portray layers of different themes (e.g., slope, aspect of surface, and drainage).

Over the last three decades this methodology has been reinforced by the rapid advancement in computer science, satellite imagery, and "Light Detection and Ranging (LiDAR) technology" (Dikau et al. 1991; Moore et al. 1991; Wilson and Gallant 2000; Dragut and Blaschke 2006; Salcher et al. 2010). High-resolution satellite imagery is widely and freely available from various agencies (e.g., "the European Space Agency – ESA", and the "United States Geological Survey – USGS"). The sensor that is used to collect LiDAR data can be mounted onto aircrafts or Unmanned Aerial Vehicles (UAV) and can produce high-resolution data with a vertical accuracy of centimeters.

In addition to the advances in remote sensing, open-source Geographical Information Systems (QGIS), as well as proprietary GIS (ArcGIS), are also contributing to Geosciences. Each GIS has its own specialty, but both have the same goal, to give a means of gathering, creating, analyzing, visualizing, and managing data. Advances in GIS have led Bonham-Carter (2014) to emphasize the significance of this tool in geosciences and how it can be applied to practical problems that involve spatial data analysis and modelling. Remote sensing data as well as LiDAR data can now produce high-resolution

(less than 1 meter) Digital Elevation Models (DEM) that can help answer difficult research questions, for example, in "hydrologic modeling" (Beven and Kirkby 1979; Darboux et al. 2002), geomorphological modelling (French, JR 2003; Jones et al. 2007), and in soil distribution (Chaplot et al. 2006; McBratney et al. 2003).

"A DEM is a numerical representation of topography" hence its quality is critical when mapping landform distribution. A low-quality DEM "may result in the over-estimation of secondary topographic attributes" (Quinn et al. 1991; Zhang and Montgomery 1994), or in the underestimation of slope gradient (Thompson et al. 2001; Toutin 2002). Thus, it can be well argued that these high-resolution DEMs are as essential as they are a challenge to the scientific community.

Identifying glacial features in the field and digitizing them can help reconstruct former ice masses and their path of movement, but it is a slow and difficult process that can be enhanced by remote sensing and GIS as emphasized also by Clark (1997). According to Otto et al. (2018) "modern geomorphological research is inextricably linked with geospatial technology and GIS".

"It is now possible to quantify landscape morphology" (Hengl and Reuter 2008; Pike 2000), "map the spatial distribution of landforms and features" (Bolch and Kamp 2005), describe and classify landforms (Dikau and Schmidt 1999), as well as enhance and support the process of identifying features in the field and reconstructing ice masses (Clark 1997; Bishop et al. 2004).

In high altitudes of the study area, near the peaks of mountains, glaciers plucked and eroded the ground forming steep and overdeepened valleys (**cirques** or corries) that could later be filled with melted water forming **tarns** (Figure 1). With decreasing altitude, the once V-shaped valleys, which are steeper in the lower valley slopes, developed into U-shaped valleys through glacier advancement and steepening (Kohl 2001b).

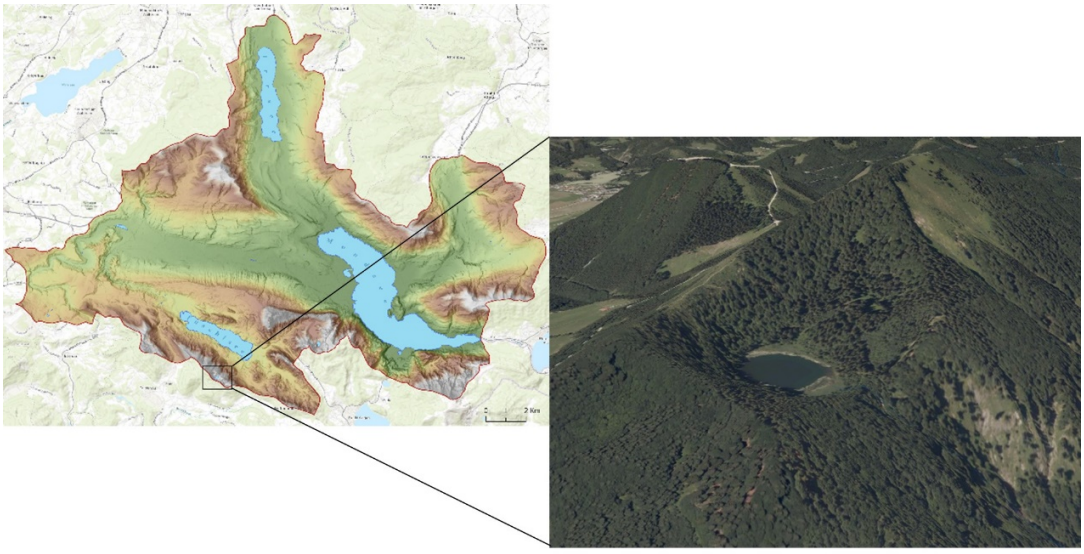

Figure 1: An example of a steep overdeepened cirque in the study area that was formed during the activity of an ice cap and later was filled with water (tarn). The image uses ESRI's World Imagery basemap.

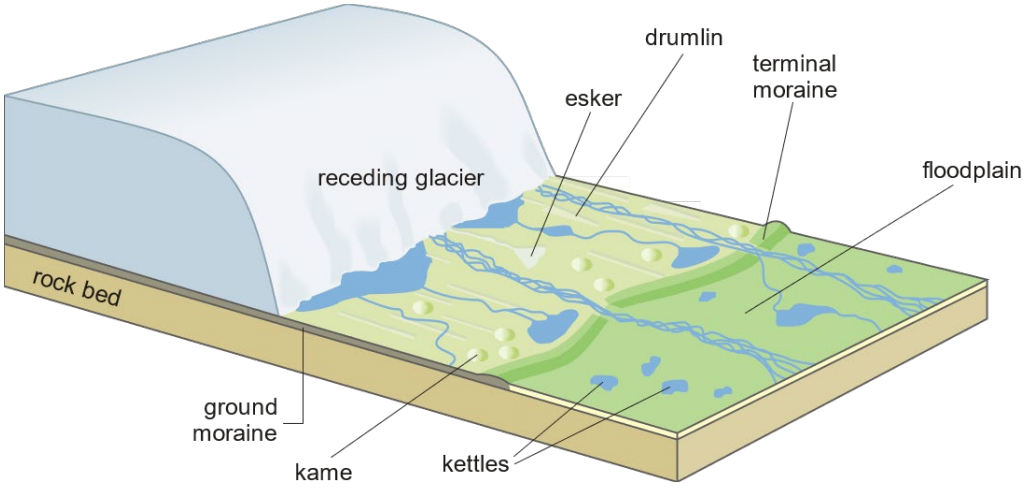

Figure 2: Signature glacial landforms formed on the outwash plain of a receding glacier. These landforms are afterward covered by other sediments and rocks or by ice masses from the glacier that started to advance again due to cold climatic conditions. However, they are easy to identify in the field even when covered. Picture by © Hans Hillewaert, CC BY-SA 4.0.

As the climate becomes warmer the ice masses retreat and melt forming outwash plains of glaciofluvial deposits and characteristic landforms. These include debris or **moraines**, either formed at the sides of the glacier's path (lateral moraines) or at the end of its path (terminal moraines), hills of irregular shape called **kames** formed by the retreat of a glacier, elongated hills called **drumlins**, and long, sinuous ridges called **eskers** (Figure 2).

Digital reconstruction and visualisation could be used for spatio-temporal educational and informational purposes. The purpose of this work is to transfer written text and graphical sketches to a visualization platform, to emphasize the importance of GIS and its contribution to a better understanding of the present geomorphological structure. This will be achieved by transferring written knowledge into the digital world with the help of GIS, showing the usability of this tool in conducting geomorphologic analysis while presenting a holistic spatial view of the origin and evolution of an area that stands for glacier activity. Sightings of glacial landforms that experts mapped in the field and mentioned in scientific papers are translated into points, lines, and polygons (Salcher et al. 2010; Dragut and Blaschke 2006), images of reconstructed ice sheets are orthorectified into raster datasets for analysis, and information on ice height is used to calculate the ice thickness by interpolation (Fischer 2009).

The digitized knowledge and the results of the analysis are presented in a Story Map that portrays a holistic view of the study area, its present geomorphology, and how it originated, via figures and interactive maps. This Story Map serves as an informational tool for hikers and adventure seekers, for example, who also want to learn more about the area. It also serves as an educational tool for students of geology or geography, for example, who can use it as a supplement while researching in the field.

2 Data and Methodology

2.1 Study Area

The study area is part of the Salzkammergut Region, covers ~247 km^2 and is located at the border of the Eastern Alps and the eastern North Alpine Foreland Basin (NAFB) in Austria. A total of around 70 lakes belong to the Salzkammergut region spreading over an area of around 2.500 km^2 and only five of them - Attersee, Traunsee, Mondsee, Wolfgangsee, and Hallstätter See - have a water surface of more than 10 km^2 (Schadler 1958). The region is generally characterized by mid-sized lakes, a dense river system, hills, and mountains (Figure 3) and its genesis and development are associated with the Quaternary Glaciation and the tectonic processes in the Alps.

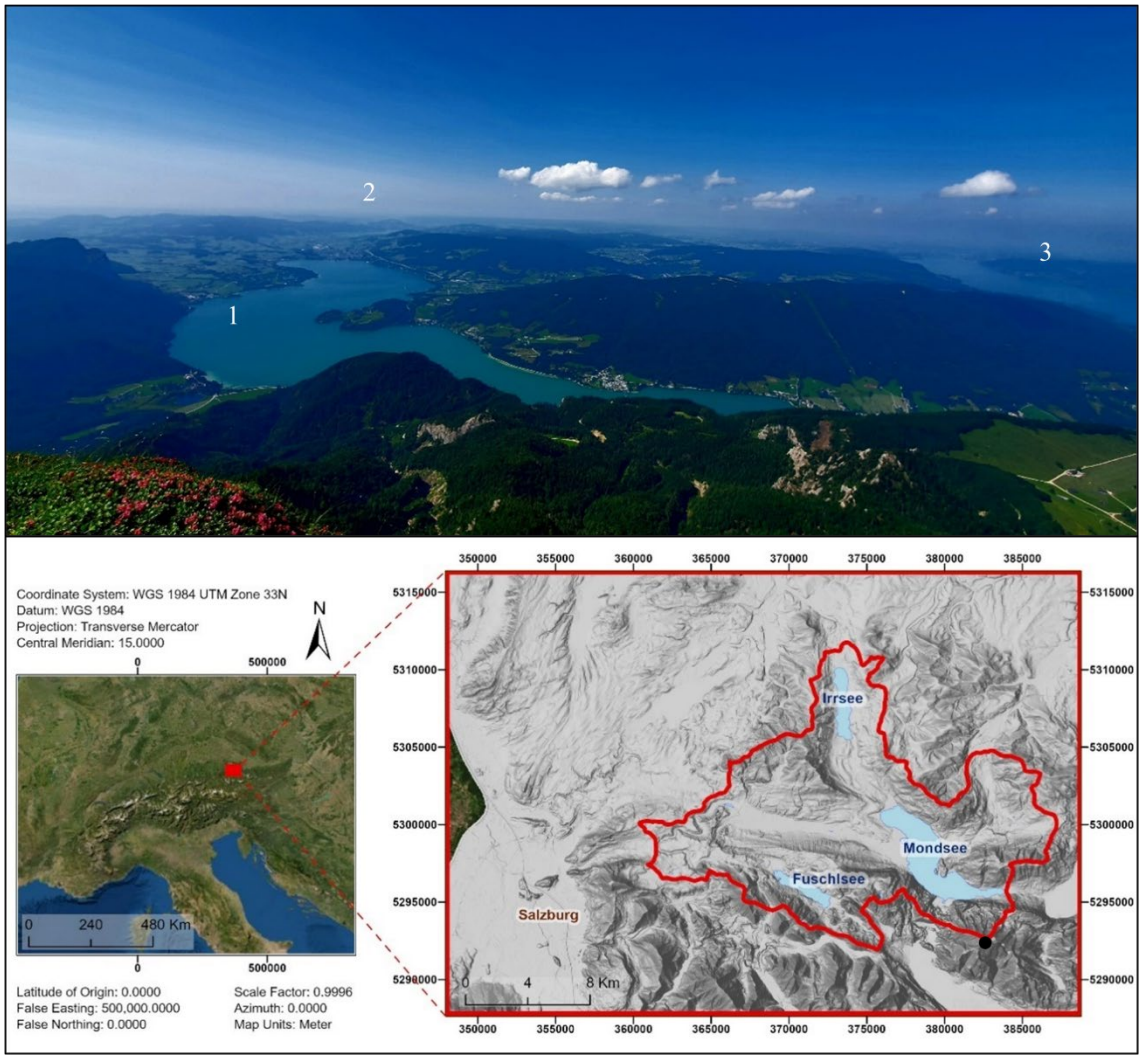

Figure 3: Location of the Mondsee Catchment Area in Austria. The photo shows (1) Mondsee Lake, (2) Irrsee Lake, and (3) Attersee Lake looking north from the summit of mountain Schafberg (black dot in the bottom right photo). Photo by: Sofia Koroxenidou

The region was covered by mighty glaciers at the start of the Quaternary period (ca. 2,6 Ma ago) that were influenced by climatic variations. Cold or "glacial" periods were

separated by warm or “interglacial” periods. The glacial periods were characterized by huge masses of ice, which during interglacial periods receded, creating signature landforms. Eventually, the conditions of the current epoch, the Holocene, which began 11.650 years ago, led to the retreat of the Alpine glaciers.

The Austrian Alps were intensively surveyed since 1800. “The first glacier inventory of the East Alpine glaciers was published by Richter (1888)”. “It was based on the 1:25.000 scale topographical maps created during the third Austrian topographic survey that was carried out from 1871 to 1873” (Rott 1993). Since 1888 the climate has changed and with it the ice cover. More recent data were made available in another inventory, “based on vertical aerial photographs taken in September and October 1969” (Patzelt 1980). There are 918 Austrian glaciers with an estimated total surface area of 540 ± 10 km^2. Another example of how advances in technology have benefited geosciences.

This work focuses on the four major glaciations that occurred in the Alps from the youngest to the oldest during the middle and late Pleistocene of the Quaternary period: “Würm, Riss, Mindel, and Günz” as they were named by Penck and Brückner (1909). The study area is uniquely shaped by the ice masses of these periods and traces of them can be well identified. The chronostratigraphic table (Figure 4) provides the stratigraphic scheme for the last 2,8 million years based on Marine Isotope Stages (MIS). These stages present the correlation between sedimentation and climatic deterioration. For a more extensive overview of the Quaternary stratigraphy of Austria, the reader is referred to Van Husen and Reitner (2011).

The *Würm* glaciation dates from 115.000 to 11.700 years ago, but this date can vary in literature as the phases between glacial and interglacial periods are assigned to one or the other period. *Riss* glaciation dates between “300.000 to 130.000 years ago and 347.000 to 128.000 years ago” (MIS 6). *Mindel* glaciation is associated with two different MIS stages, MIS 10 which dates to 374.000 – 337.000 years ago and MIS 12 which dates to 478.000 – 424.000 years ago. Of the two stages, MIS 12 is the strongest glacial and most associated with the Mindel glaciation of the alps, the Anglian glaciation of the British Isles, and the Elster glaciation of North Europe. The *Günz* glaciation in the Alps is associated with the Glacial a and b of the Cromerian Complex (MIS 16, 18, 20) and dates to 800.000 to 600.000 years ago.

It can be deduced that the Günz and Mindel glaciations which fall in the Brunhes Chron (Van Husen 2000) coincide with the global excess 100-kyr ice due to prolonged intervals of low summer insolation followed by extensive Terminations as documented in the $\delta\,^{18}O$ records of Raymo (1997). The same adheres to the Riss and Würm glaciations, but it is more verifiable due to geochronological data collected from rocks and sediments, that determine and associate their age with the glaciations. Typically, the Alpine proglacial sediments are covered by basal till and terminal moraines.

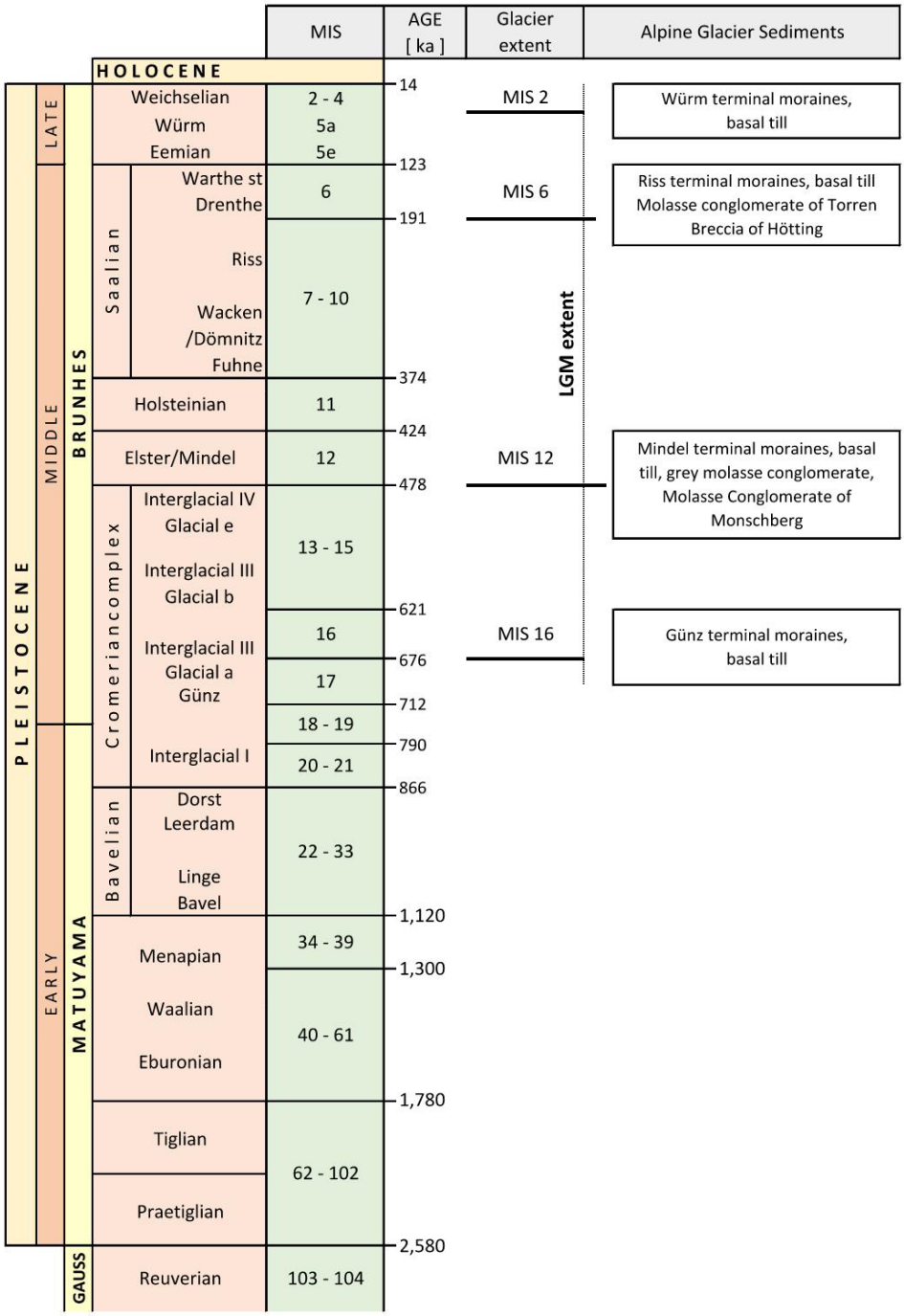

Figure 4: Table showing the stratigraphy of the Quaternary and its subdivisions in correlation with MIS stages and Alpine sediments found in Austria. The chronostratigraphic scheme is given by Gibbard and Cohen (2008) and was modified by the author of this work to include the Alpine Sedimentary units of Austria during the four major glaciations. The modifications were made after Van Husen and Reitner (2011). The glacier extent represents the known extent of the glaciers for the duration of the Brunhes Chron. The LGM extent represents the Last Glacier Maximum during the Würm glaciation.

The Alpine orogenic process started in the Palaeozoic million years ago and continues to this day. It is a product of two orogens, the first took place in the Cretaceous and the second in the Tertiary (Froitzheim et al. 1996; Schmid et al. 2004; Meschede 2015). The long-existent supercontinent consisting of one tectonic plate, Pangaea, began to break

apart during the Mesozoic about 200 Ma ago due to rifting processes from the opening of the North and South Penninic oceans. The first collision occurred in the Jurassic at the North end of Neotethys and later began the subduction at its margin. The subduction of the Penninic Oceans in the late Cretaceous ultimately led to the collision of the Adriatic Plate with the European Plate in the early Tertiary causing obduction, characteristic nappes, thrust faults, tectonic windows, and the eventual forming of the Alpine orogenic belt. Due to this convergence, the European Alps mark "the closure of ocean basins in the Mediterranean" (Frisch 1979; Trümpy 1960).

The study area is affected by this compression due to stress and pressure at the convergent boundary with tectonic uplift. It can be subdivided into "two geological units by a **Tertiary thrust fault** along the southern shoreline of lake Mondsee" (Van Husen 1989b). The northern part, which covers ~70% of the catchment, is defined by Late Cretaceous sediments of the "Rhenodanubian" Flysch zone; a term used because this zone is located between the rivers Rhine and Danube (Tichy 2000). It is characterized by gentle slopes that reach an elevation of no more than 1.000 m. The southern part, which covers ~30% of the catchment, is defined by Triassic and Jurassic carbonate rocks such as limestone, and dolomite of the Northern Calcareous Alps that form steeper slopes reaching an elevation of 1.782 m, the mountain Schafberg (Figure 5).

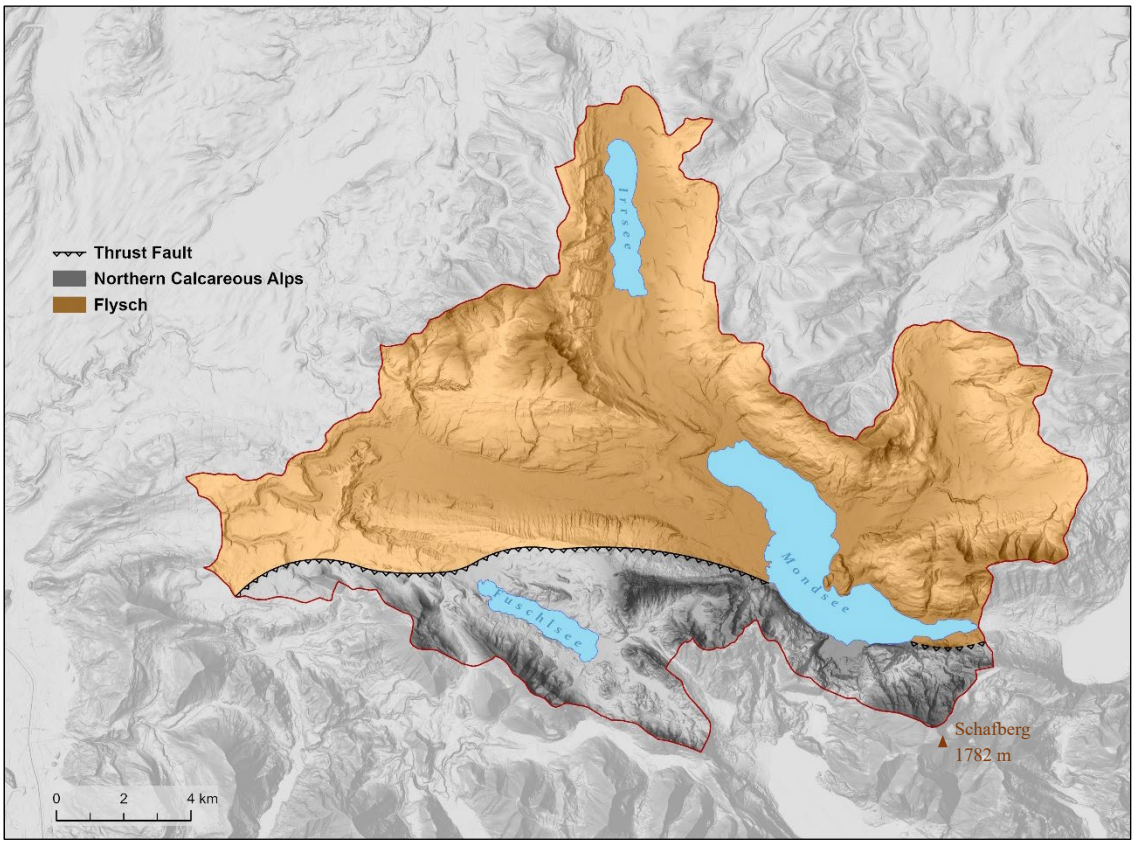

Figure 5: Mondsee Catchment showing the two geological units, the Northern Calcareous Alps, and the Flysch zone, divided by the thrust fault.

Every lake of Salzkammergut is closely related to the erosion caused by glaciers during the current and youngest Period of the Geological Time Scale, the Quaternary. It includes the Pleistocene and Holocene Epochs and spans from 2,6 Ma ago to the present day. The cold climate during this Period helped form **piedmont** glaciers in the valleys that today are covered by flora and fauna and inhabited by mankind. This type of glacier characterizes a large part of the Eastern Alps and is formed when a **valley** glacier exits a deep and confining bedrock valley and spreads outwards in the shape of a lobe. These glaciers slowly eroded the bedrock, creating basins that trapped the melting water, forming the lakes.

Lake Irrsee (47°54'40"N, 13°18'30"E, 553 m above sea level; asl) exists in a transverse valley trough in the Flysch zone and drains the northern catchment to the South via the Zeller Ache stream, one of the main tributaries of lake Mondsee. The other being the Wangauer Ache and the Griesler Ache/ Fuschlerache (Figure 6). Lake Mondsee (47°49'30"N, 13°23'20"E, 481 m asl) lies in the marginal trough of the Calcareous Alps and Flysch zone and has a maximum depth of 68 meters. “The lake basin has been substantially altered by the Pleistocene glaciations” (Kohl 1998; Van Husen 1989b). Fuschlsee (47°48'2"N, 13°18'45"E, 663 m asl) lies in the southern part of the study area in the Calcareous Alps zone and has a depth of 67 meters (Table 1).

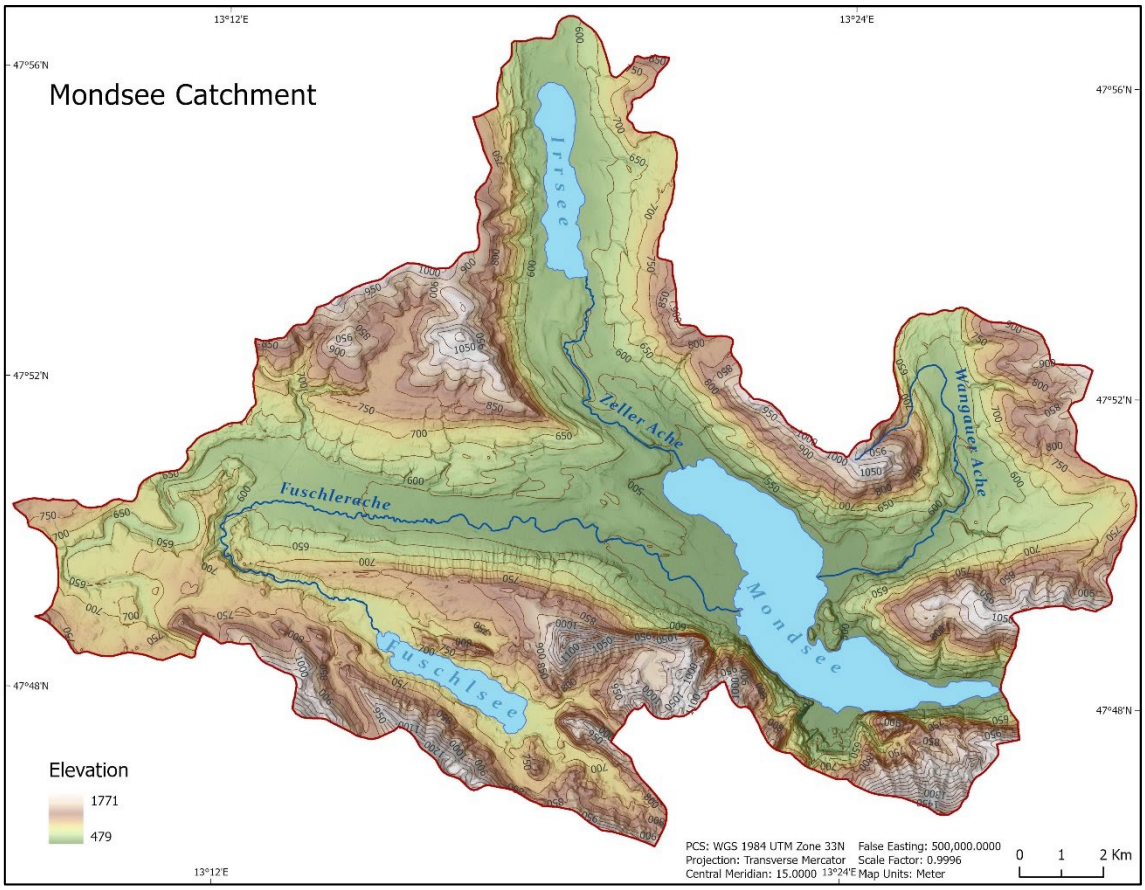

Figure 6: Mondsee Catchment showing the elevation of the area and the main tributaries of Mondsee lake; Zeller Ache, Wangauer Ache and Griesler Ache/Fuschlerache.

Name	Meters above sea level	Maximum Depth (m)	Size (km^2)	Catchment (km^2)
Irrsee	553	32	3,6	28
Mondsee	481	68	13,8	247
Fuschlsee	663	67	2,7	30

Table 1: Table showing the biggest lakes in the study area, their maximum depth, their size, catchment area size, and the meters above sea level of each lake after Beiwl and Mühlemann (2008) and Beiwl and Rodinger (2010).

Penck and Brückner (1909) proposed a four-glaciation theory to subdivide the Quaternary and named each period after the southern German rivers: "Günz, Mindel, Riss, and Würm" based on a vertical fluvial terrace that was broadly utilized in the last century. Their theory describes the "classical" Alpine Stratigraphy and suggests that the tongue basins are connected to terminal moraines, gravels, and terraces comprised of proglacial outwash – from younger to older: "Niederterrasse (Würm), Hochterrasse (Riss), Jüngerer Deckenschotter (Mindel), Älterer Deckenschotter (Günz)".

"The terraces and moraines of the four glaciations differ in terms of the degree of weathering and the characteristics of the cover beds, for example, loess" (Van Husen and Reitner 2011). The Niederterrasse (low terrace) was initially identified as the lowest of the river terraces and "later considered to be an accumulation of the meltwater from the last glacial period", Würm (Penck and Brückner 1909). "Its deposits consist of coarse, sand-bearing gravel with weak bedding" and can be located northeast of Irrsee and northwest of Attersee (Van Husen and Reitner 2011).

The Salzkammergut was filled by the Traun glacier as far as the northern boundary of the Alps and beyond. It covered the basins of lakes Traunsee and Attersee, east of the study area, the basin of Mondsee, and the basin of Irrsee. During the Mindel glacial period, the glacier advanced northwest to the southern foothills of the Kobernaußerwald mountain near Straßwalchen and Frankenmarkt and in the Würm period, it left closed terminal moraines (Van Husen 2003; Kohl 2001a).

Another mighty glacier is the Salzach glacier that followed the Saalach and Salzach valleys – now rivers – to the north where the two ice streams merged in the city of Salzburg and formed a foreland glacier. From the basin of Salzburg, it fanned out into several branch basins. During the Würm High Glacial (~20.000 years ago) it extended over an area of 6.000 km^2 (Horst Ibetsberger 2003). This glacier's activity covered the west side of the study area.

The Salzach glacier left behind ground moraines and terminal moraines from the Würm, Riss, and Mindel glacial periods, of which the Würm moraines exceeded the Riss moraines several times. The Salzburg Nagelfluh – tertiary conglomerate – an interglacial delta formation suggests that an interglacial lake with a length of 30 km, a width of 10 km, and a depth of 0-8 km existed in the basin of Salzburg (Penk and Brückner 1902).

The rivers that drained into the lake transported clay-rich rock debris such as micaceous schist, phyllite, gneiss, etc. from the central Alps. This led to the rapid filling of the lake ca. 13.000 years ago (Horst Ibetsberger 2003).

Observing the terrain of the study area and its surroundings one can observe the glacial landforms created by the glaciers and many water bodies (Figure 7). The Salzach glacier, which flowed North through the Salzburg foreland, formed U-shaped tunnel valleys underneath the ice (Weinberger 1952), but also Drumlins, Eskers, and Kames (Kohl 2001b). Kettle holes formed also frequently and, in some cases, the remaining ice formed small lakes in the terminal basin of the glacier (Kohl 2001b) that are visible in Figure 7.

There were also bigger lakes formed due to the ploughing of the Salzach glacier. The basin of lake Wallersee was formed this way and today is surrounded by terminal moraines of the Würm glaciation (Schaber 2015) and it is there that the Wenger moor was also formed and was listed since 1995 as a Natura 2000 European protection area since it is the home of many Biotopes. Lakes Mattsee, Obertrumersee, and Grabensee (top left in Figure 7) were once a single lake, the Urmattsee lake, which was formed due to the melting of Mattsee glacier (branch of the Salzach glacier) between 18.500 and 18.000 BC (Seefeldner 1961). Seefeldner (1961) explains the reason for the tripartition of this grand lake. After the lake level reached ~510 m asl it levelled off around 10.000 BC, when the Mattig river created drainage through the terminal moraines north of Grabensee which led to the lowering of the water level and ultimately to the tripartition into three lakes.

Figure 7: Mondsee Catchment and surrounding area hillshade overlayed on a basemap (www.basemap.at).

Another area of interest southwest of the Mondsee catchment is the municipality of Koppl (Figure 8), which will be further discussed in chapter 2.1.1. The overload of the glacier in Koppl reached 40 kp/cm^3 during the last glaciation giving the silt and clay rocks a compact appearance and a very high bulk density and leaving ground moraines that formed a landscape with wet meadows, ponds, and moors (Tichy 2000) like the Koppler moor (Figure 9). The glacier extended its branches – the Wiestal, and the Guggenthal branch – that played a significant role in the area (Weinberger 1955) and left also terminal moraines behind. After the ice melted Kames, and Eskers were formed.

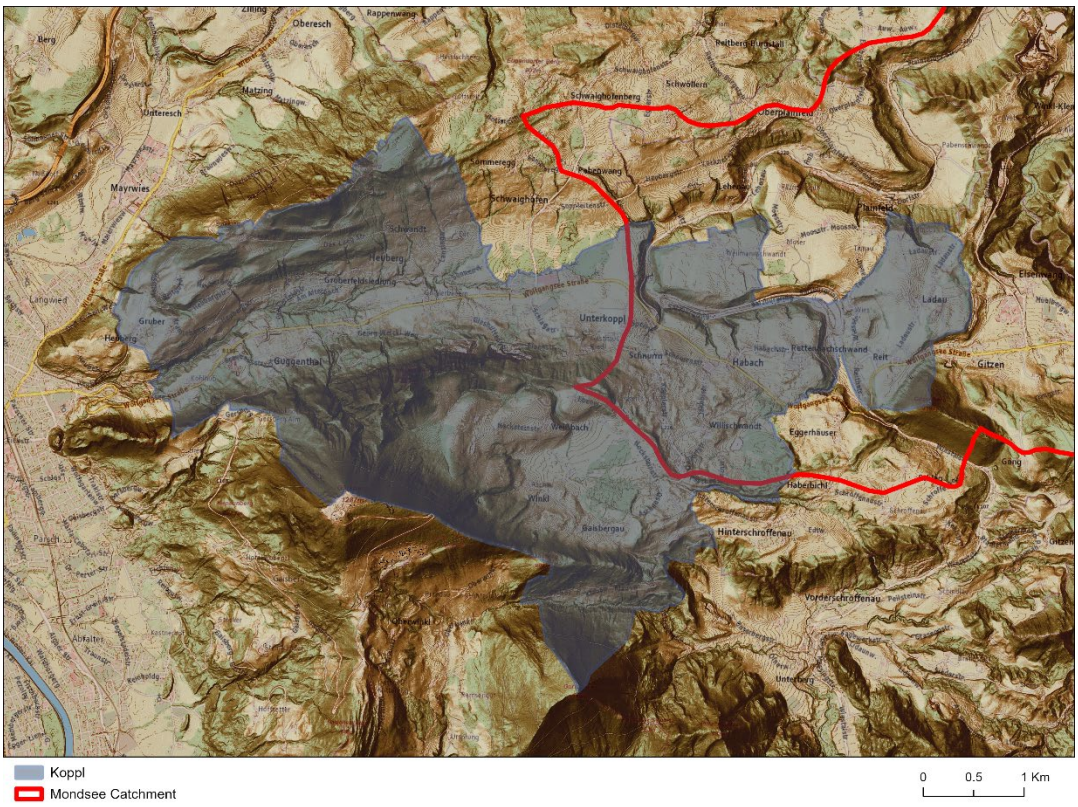

Figure 8: Koppl municipality hillshade overlayed on a basemap (www.basemap.at).

Figure 9: Koppler Moor with its dense vegetation.

2.1.1 Würm Glaciation

The Würm glaciation is the last Alpine glaciation and is "divided into three phases, early, middle, and late". The early phase is characterized by depositions of gravel, and moraines, the middle by three systems of moraines and outwash fans, after the glaciers reached their maximal stand and covered the previous deposits, and the late phase by the melting of the glaciers and the creation of big lakes (Ebers 1955). There are three glacier levels that are generally distinguished today: an inner, a middle (Hochstand), and an outer level (Maximalstand) (Weinberger 1955).

About 20.000 years ago the equilibrium line altitude (ELA) was about 1.200 meters lower than it is today (Kohl 2001a). This line signifies the altitude at which the accumulation of snow is equal to the melting of snow (ablation zone) and depends not only on low temperatures but also on strong precipitation. When the ELA is low, a considerable amount of snow accumulates in the mountains and long and extended glacier tongues are formed in the valleys (Figure 10).

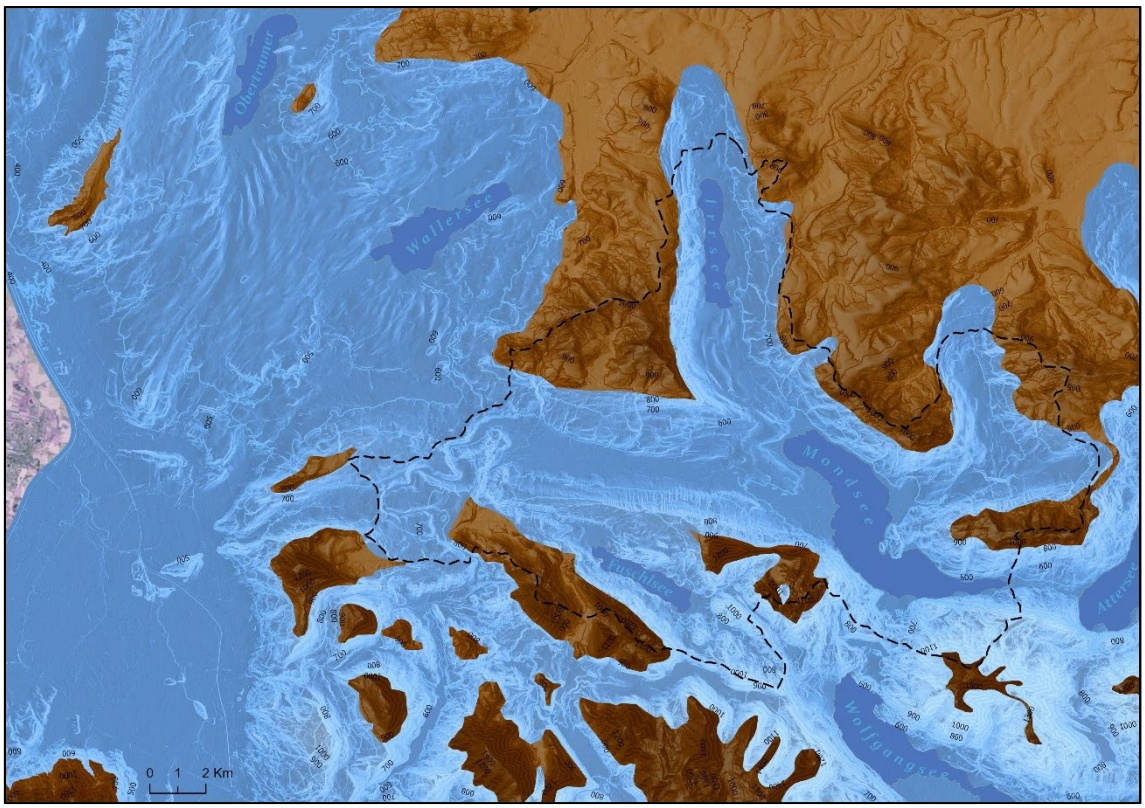

Figure 10: Reconstruction of the Würm maximum glaciation modified after Egger and Van Husen (2009) and Egger and Van Husen (2014). The dashed black line defines the Mondsee catchment.

The catchment area is covered by the Salzach and the Traun glacier from the west and from the east respectively. The mountains along the boundaries are ice-free, and the ice streams flow in the valleys among them. During the Würm glaciation, the Salzach glacier covered an area of 6.500 km^2 (Brückner 1886). The mighty common terminal moraine of the Salzach, Traun and Hintersee glaciers runs through the center of Faistenau as shown in Figure 11 (Van Husen 1989a).

In the first phase of the late glacial ice melting, Hinterschroffenau near Koppl was filled with a lake that drained north over the Plainfeld stream until it dropped to 690 m (Ebers et al. 1966; Meneweger 1993). According to Seefeldner (1961) the "accumulating activity" of the Salzach glacier is presumed to be significant in Koppl, and evident by its two branches: the *Wiestal* branch, whose terminal moraines cover the tongue basin of Ebenau in a large arc, beginning in the Hinterschroffenau, inverting into the Vorderschroffenau, where they were, of course, largely cut off by the streams flowing centripetal towards the middle of the tongue basin; and the *Guggenthal* branch advancing north of mountain Gaisberg, the outermost moraines of which run from the east end of the Nockstein range in a large semicircle via Koppl-Ladau to Wassenegg (Figure 11).

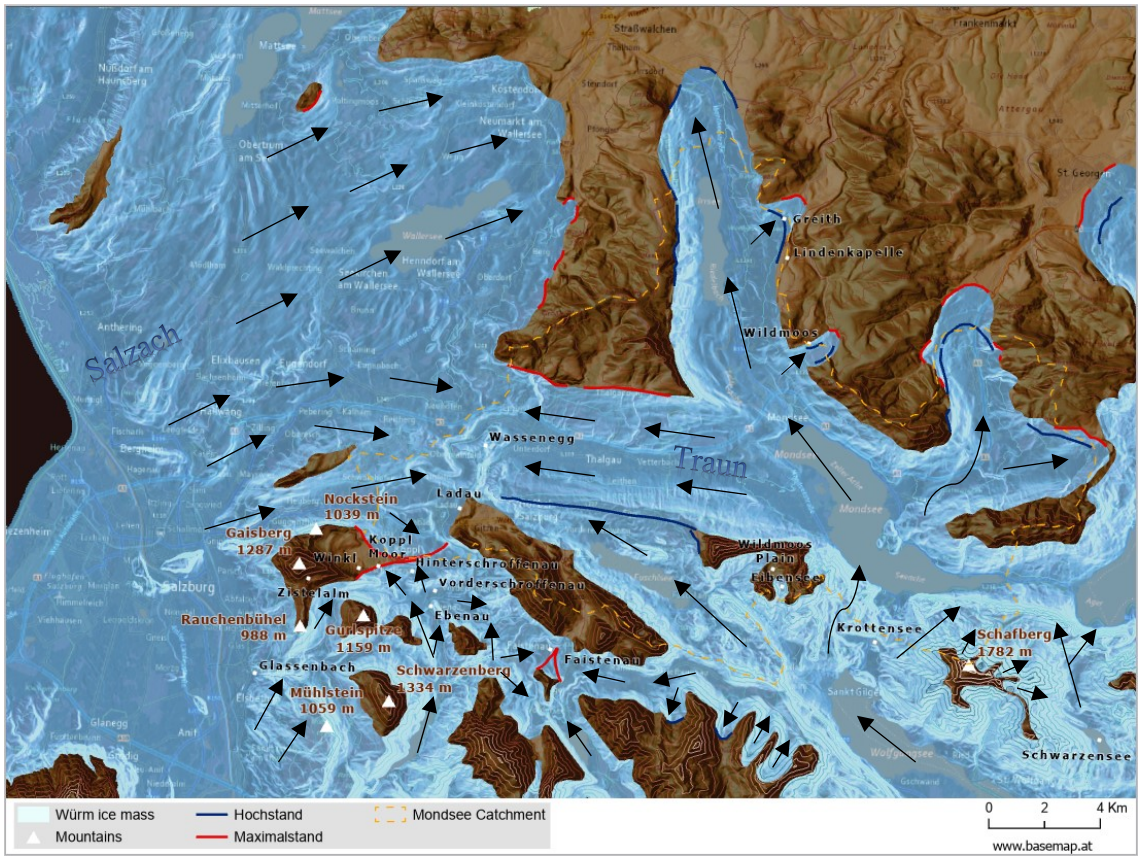

Figure 11: Flow paths of the Salzach and Traun glaciers from the west and east respectively modified after Egger and Van Husen (2009) and Egger and Van Husen (2014).

Regarding the Würm moraines of the Guggenthal branch of the Salzach glacier, sightings of Gosau erratics are very frequent, and were transported there from the west side of Gaisberg (Seefeldner 1961; Meneweger 1993). Between the two moraine walls that almost touch at Koppl on the one hand and the foothills of the Gaisberg and Nockstein ranges on the other, lies the Winkl basin; in it, as glacial varves (annual sediment layers) prove, an ice reservoir was formed during the Würm glaciation. Today this reservoir is occupied by a raised bog (Highmoor), the Koppler moor as shown in Figure 11.

Götzinger (1958) mentioned that the Würm glaciation at Gaisberg ice near Zistelalm had over ***900 m*** asl height. Authors after Götzinger such as Seefeldner (1961), and Ebers et

al. (1966) confirmed this height. Del-Negro (1957) reports individual observations. He confirms the moraines at Zistelalm, mentions erratics to the east up to an altitude of more than ***1.000 m***, mighty moraine walls between the Rauchenbühel and Gurlberg mountains, and on both sides of the Glassenbach gorge, and between the mountains Mühlstein and Schwarzenberg (Figure 11). The Gersberg trough, NW of Gaisberg, extends over an altitude of about 700 to 900 m; the Rauchenbühel reaches up to ***988 m*** (Gamerith and Heuberger 1990). Van Husen (1987) mentions the height of the ice flow on the north side of Gaisberg at ***1.000 m*** and on the south side at almost ***1.050 m***.

The east part of the catchment was covered by the ice masses of the Traun glacier that divided at Bad Ischl (SE of Lake Wolfgang) into a branch that flowed toward Attersee, and one that flowed through the furrow of Lake Wolfgang. From the latter branch, which was also fed with ice from Postalm (N of Lake Wolfgang), large masses flowed northwards via the furrows at Schwarzensee to the east and at Krottensee to the west of mountain Schafberg, while a smaller branch advanced to the basin of Lake Fuschlsee (Figure 11). The latter penetrated the valley of the Eibensee river up to a height of approx. ***950 m*** and blocked the valley, resulting in the Wildmoos plain (Figure 11). From the south, however, an ice tongue had also entered the valley of the Eibensee via the saddle at the Eibensee alp. The small tongue basin lake was formed within its terminal moraine (Egger and Van Husen 2014). Lichtenecker (1938) describes this lake as an outcome of a cirque glacier and not as a moraine-dammed lake as described above by Egger and Van Husen (2014).

The large ice masses filled the basins of Lakes Attersee and Mondsee, penetrated deep into the valley of the Wangauer Ache and formed glacier tongues in Thalgau and Irrsee (Egger and Van Husen 2003). The glacier tongue at Lake Mondsee was in the Ablation area of the Traun glacier (Van Husen 1987) with a snow line that reached around ***1.100 m*** (Lichtenecker 1938). Other local cirque glaciers indicate that the snow line was between ***1.050 m*** for the Eibensee glacier, ***1.150 m*** for the Filbling glacier, and 1.000 m for the Laudachsee glacier, east of Lake Attersee (Lichtenecker 1938).

The south and east parts of the glacier lobes at lake Irrsee were mapped in 1982. The lake`s basin is filled with massive ground moraines originating from Traun glacier forming a closed blanket with clear drumlin formation. The eastern edge of the Würm Traun glacier tongue of the Irrsee branch is marked by an almost complete terminal moraine line. A clear wall encloses the small tongue basin of Wildmoos. A mighty wall of terminal moraines is formed from Lindenkapelle to Greith (Figure 11). In the area south of Lindenkapelle there are many preserved kettle holes (Van Husen 1982).

In 1983 the west bank of lake Attersee and the municipality of Oberwang, between lake Mondsee and lake Attersee were mapped. In his report, Dirk Van Husen (1983) describes a short maximum extent (“Maximalstand”) and a prolonged high extent (“Hochstand”) that can be seen “in the Oberwang tongue basin of the Traun glacier”. The Hochstand is

marked with mighty moraines that cross the valley of Stadlpoint. The line follows the course via Grossenschwandt - Riedschwandt - Schernberger - Kulmbauer developed as a closed wall up to Konradskapelle (Figure 12). The higher line that goes around Schernberger, Bergschuster all the way to Schwaighof marks the Maximalstand moraines (Van Husen 1983).

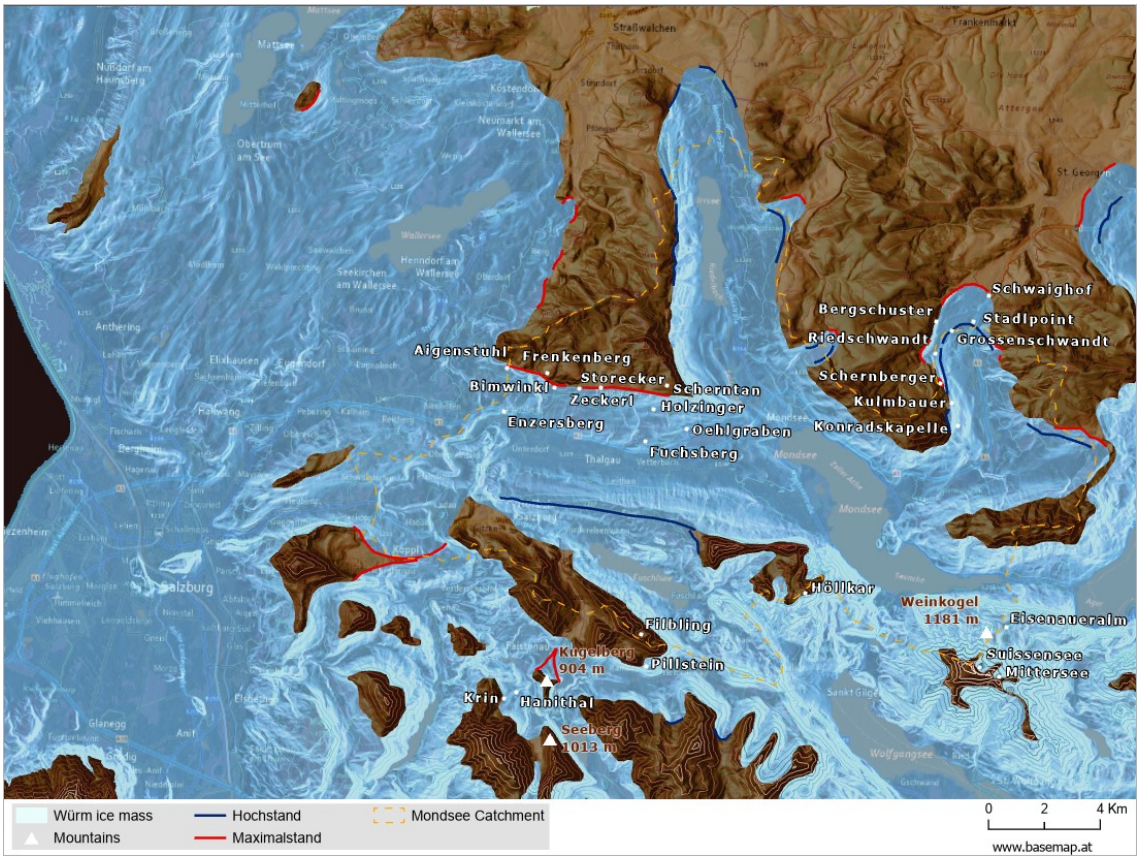

Figure 12: Traun glacier ice reconstruction modified after Egger and Van Husen (2009) and Egger and Van Husen (2014) regarding the area west of Attersee, Thalgau basin, N of Schafberg, and S of Fuschlsee.

In 1985, Van Husen (1985) described well-developed lateral moraines left behind by the Traun glacier on the northern edge (Thalgauberg) of the Thalgau basin. This started at 840 m below Scherntan and continued via Storecker - Zecherl - Bimwinkl to Aigenstuhl (Figure 12). The lateral moraines of Aigenstuhl represent the easternmost moraines of the Salzach Glacier. The ice masses formed powerful terraces to the side valleys, which are about ***700 m*** high west of Frenkenberg and about ***750 m*** high near Wasenmoos, east of Frenkenberg. The lower areas of the Thalgauberg were clearly formed and shaped from the ice (sheepbacks near Oehlgraben, Fuchsberg, Holzinger) or they are covered with ground moraines (Figure 12). Further to the south, a terrace of ***1.040 m*** height east of Lake Filbling marks the height of the ice. Further to the east of Lake Fuschlsee, the ice reached a height of approx. ***1.100 m*** at Höllkar, where it divided into the Mondsee branch to the north and the Fuschlsee branch to the west. The ice masses advanced northwards via the Eibensee branch and stored the approx. 30 m thick moraine that dams the Eibensee. Ice flow is noticed coming also from the Wolfgangsee basin forming a glacier

tongue. Its height is indicated by a terrace and a moraine wall at Pillstein on the north side at ***940 m*** (Van Husen 1985). On the south side of Pillstein, above the mountain lodge, he mentions a ***985 m*** moraine, a high, wide wall at ***1.040 m***, and a narrow one at ***1.060 m*** formed by the Traun glacier branches differentiating between a high (Hochstand) and a maximum extent (Maximalstand) (Figure 12). These terminal (lateral) moraines of the tongue basin of the Thalgau glacier branch come in contact at Enzersberg with the end moraines of the Salzach glacier, namely the Söllheim-Kraiwiesen tongue basin (Götzinger 1958).

South of mountain Kugelberg, the Salzach and Hintersee glaciers came into contact (Van Husen 1989a). He sees the end of the Salzach Glacier further advanced to the terminal moraines west of Seeberg. However, according to Meneweger (1993), the fact that the ice did not reach this height of 825 m and that the glacier must have advanced disproportionately far in comparison to Faistenau defies this large extent. Meneweger (1993) reinforces this opinion due to the glacial terraces at Hanithal and Krin, and their position and height (Figure 12).

Van Husen (1986) describes a succession of moraines that has been preserved around the Eisenauer Alm, which were deposited by the ice tongues from the cirques of the Suissensee and Mittersee lakes. He also mentions the mighty wall east of Weinkogel, which marks the western limit of the ice flow, and shows the highest level of ice (Van Husen 1986) (Figure 12).

Finally, Götzinger (1957) described in his report the terminal and lateral moraines in Koppl along with their height in meters asl. He mentioned the following series of lateral moraines that can be observed from bottom to top from the Heuberg hillside (in meters asl): "Pabenwang ***745***, Sommeregg ***765***, Haring ***772***, Hochfuchs-Schopper ***799***". Hence there are four retreat phases of the glacier in the Würm and in the Würm Late Glaciation. Götzinger (1957) also mentioned lateral and terminal moraines at Koppl ***753***, Weißbach ***810***, and Gaisbergau ***776*** among other locations that can be found in Table 2 and Figure 13.

Table 2: Glacial landforms sightings of the Würm glaciation as reported by scientists. M: Moraine, LM: Lateral Moraine, TM: Terminal Moraine, LM/TM: Lateral/Terminal Moraine, E: Erratics, H: Height information, T: Terrace, SL: Snow Line.

	LOCATION	HEIGHT	TYPE	AUTHOR	LATITUDE	LONGITUDE
1	Sommeregg	765	LM	Götzinger 1957	5299579	360100
2	Pabenwang	745	LM	Götzinger 1957	5299474	360977
3	Haring	772	LM	Götzinger 1957	5300137	360860
4	Hochfuchs-Schopper	799	LM	Götzinger 1957	5300692	360488
5	W of Kapaunberg	680	LM	Fugger and Kastner 1885	5296242	357228
6	Zistelalm	1000	LM	Götzinger 1936	5295705	359073
7	Sattel	947	LM	Götzinger 1936	5294805	359064
8	East ridge of Gaisberg	1000	E	Götzinger 1930	5295893	360005
9	E of Zistelalm	1000	E	Del-Negro 1957	5295723	359332
10	Above the city of Salzburg	1050	H	Brückner 1886	5297317	353197
11	Gaisbergau	776	M	Götzinger 1957	5295938	360815
12	Weißbach	810	M	Götzinger 1957	5297199	360645
13	Koppl	753	LM	Götzinger 1957	5296638	361854
14	South of Gaisberg	1050	M	Van Husen 1987	5295534	358657
15	North of Gaisberg	1000	M	Van Husen 1987	5296840	358529
16	South of Heuberg	800	M	Götzinger 1958	5299095	358410
17	North of Heuberg	800	M	Götzinger 1958	5299507	358317
18	E of Kraiwiesen	650	M	Götzinger 1958	5301927	365063
19	Western slope of Große Plaike	680	M	Götzinger 1958	5305546	367016
20	Eastern slope of Buchberg	700	M	Götzinger 1958	5312731	359270
21	Southern slope of Tannberg	680	M	Götzinger 1958	5314291	364856
22	Neumarkt	570	TM	Götzinger 1958	5311719	366882
23	N of Haunsberg	760	M	Götzinger 1958	5309090	350495
24	Buchberg slope	660	M	Götzinger 1958	5313141	358468
25	Northern slope of Tannberg	600	M	Götzinger 1958	5316073	363672
26	Gottsreit	822	M	Götzinger 1957	5300370	359638
27	NW Sommeregg	811	M	Götzinger 1957	5299615	359630
28	Wassenegg	724	TM	Götzinger 1957	5300473	365299
29	Strickbichl	754	TM	Götzinger 1957	5298049	364672

	LOCATION	HEIGHT	TYPE	AUTHOR	LATITUDE	LONGITUDE
30	E Elsenwang	730	M	Götzinger 1957	5298099	366047
31	Heuberg slope	860	LM	Götzinger 1957	5299330	358372
32	Heinisberg	724	LM	Götzinger 1957	5300700	359540
33	Rappenwang	651	LM	Götzinger 1957	5301121	359278
34	Gersbach-Hub	590	LM	Götzinger 1957	5305803	363973
35	Stallergut	652	LM	Götzinger 1957	5304675	364902
36	SE Stallergut	669	LM	Götzinger 1957	5304489	365091
37	Gräbl	654	LM	Götzinger 1957	5313169	359552
38	Untermayerhof	675	LM	Götzinger 1957	5312404	359446
39	Obermayerhof	675	LM	Götzinger 1957	5312456	359214
40	Rettenschwand	711	TM	Götzinger 1957	5297693	363260
41	Lackner	700	TM	Götzinger 1957	5299931	362660
42	Römersberg	640	LM	Götzinger 1957	5313449	358451
43	Pfaffenberg	579	LM	Götzinger 1957	5313717	358058
44	N of Haberbichl	772	LM/TM	Götzinger 1957	5296620	363348
45	Riedl	690	LM	Götzinger 1957	5297942	361050
46	N edge of Lake Wolfgang	1100	SL	Lichtenecker 1938	5289288	375789
47	N edge of Lake Wolfgang	1100	SL	Lichtenecker 1938	5292503	381446
48	Eibensee cirque glacier	1050	SL	Lichtenecker 1938	5295137	375891
49	Filbling cirque glacier	1150	SL	Lichtenecker 1938	5293711	370862
50	W of Frenkenberg	700	LM	Van Husen 1985	5303133	366441
51	Near Wasenmoos	750	LM	Van Husen 1985	5302583	369348
52	Höllkar	1100	LM	Van Husen 1985	5295082	376864
53	E of Filblingsee	1040	M	Van Husen 1985	5293703	371597
54	N of Pillstein	940	M	Van Husen 1985	5292865	371190
55	S of Pillstein	985	LM/TM	Van Husen 1985	5290640	372136
56	S of Pillstein	1040	LM/TM	Van Husen 1985	5290278	372167
57	S of Pillstein	1060	LM/TM	Van Husen 1985	5290058	372159
58	E of Weinkogel	1050	M	Van Husen 1986	5293954	383722
59	Above the city of Salzburg	1050	H	Brückner 1886	5295691	353843
60	Above the city of Salzburg	1050	H	Brückner 1886	5293419	353319

	LOCATION	HEIGHT	TYPE	AUTHOR	LATITUDE	LONGITUDE
61	Below Scherntan	840	LM	Van Husen 1985	5302259	371841
62	Wasenmoos	750	LM	Van Husen 1985	5302859	368537
63	Grossenschwandt Hochstand	630	TM	Deduced after Van Husen 1985	5304614	382048
66	Riedschwandt Hochstand	655	TM	Deduced after Van Husen 1985	5303788	381474
67	Kulmbauer Hochstand	720	LM	Deduced after Van Husen 1985	5302029	382030
68	Schernberger Hochstand	640	LM	Deduced after Van Husen 1985	5302713	381845
69	Bergschuster Maximalstand	650	TM	Deduced after Van Husen 1985	5304941	381500
70	Schwaighof Maximalstand	600	TM	Deduced after Van Husen 1985	5305851	383381
71	Krin Terrace	770	T	Deduced after Meneweger 1993	5291471	366055
72	Hanithal Terrace	750	T	Deduced after Meneweger 1993	5291681	366454
73	Brunnfeld	850	H	Deduced after Egger & Van Husen 2014	5296735	384332
74	Petershöhe	850	H	Deduced after Egger & Van Husen 2014	5298722	385848
75	Above Radau Hochstand	750	H	Deduced after Egger & Van Husen 2014	5300856	385628
76	Geiselstatt	770	H	Deduced afer Egger & Van Husen 2014	5301074	386464
77	Wildmoos	800	TM	Deduced after Van Husen 1982	5303999	376921
78	Hochmoos	800	TM	Deduced after Van Husen 1982	5303807	377590
79	Maximal stand east of Wildmoos	780	TM	Deduced after Egger & Van Husen 2014	5304507	377830
80	Greith Hochstand	700	TM	Deduced after Van Husen 1982	5308690	376125
81	Lindenkapelle	720	TM	Deduced after Van Husen 1982	5307228	375998

	LOCATION	HEIGHT	TYPE	AUTHOR	LATITUDE	LONGITUDE
82	W of Fischhof Hochstand	700	H	Deduced after Egger & Van Husen 2014	5309467	372155
83	Haslach Hochstand	580	H	Deduced after Egger & Van Husen 2014	5313007	372203
84	Winzerroid Hochstand	620	H	Deduced after Egger & Van Husen 2014	5313129	374095
85	Pirach Hochstand	560	H	Deduced after Egger & Van Husen 2014	5313960	373090
86	W of Schwarzenberg	900	H	Deduced after Egger & Van Husen 2014	5290671	361109
87	E of Schwarzenberg	900	H	Deduced after Egger & Van Husen 2014	5291325	362553
88	Mühlstein	1060	H	Deduced after Egger & Van Husen 2014	5290366	359601
89	Aichereben	750	H	Deduced after Egger & Van Husen 2014	5299971	387443

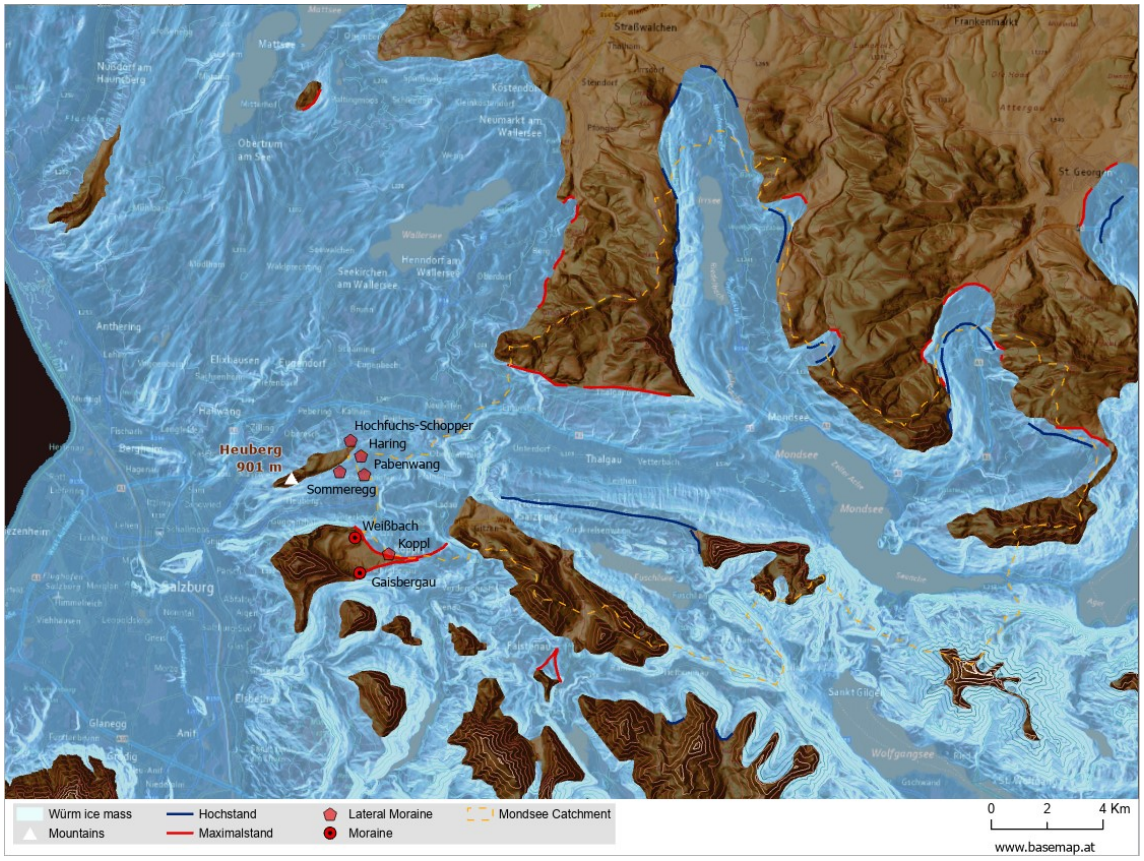

Figure 13: Würm ice reconstruction modified after Egger and Van Husen (2009) and Egger and Van Husen (2014) regarding Koppl and the report by Götzinger (1957).

2.1.2 Riss Glaciation

This is the penultimate glaciation with an equilibrium line altitude (ELA) 100 meters lower than that of the last glaciation, Würm (Penck and Brückner 1909). This indicates larger accumulation zones in the mountain areas and extensive glacier tongues in the valleys (Figure 14). Today, the moraine walls are generally divided into two events with their own glacial till that formed terraces (Weinberger 1955; Del Negro 1967).

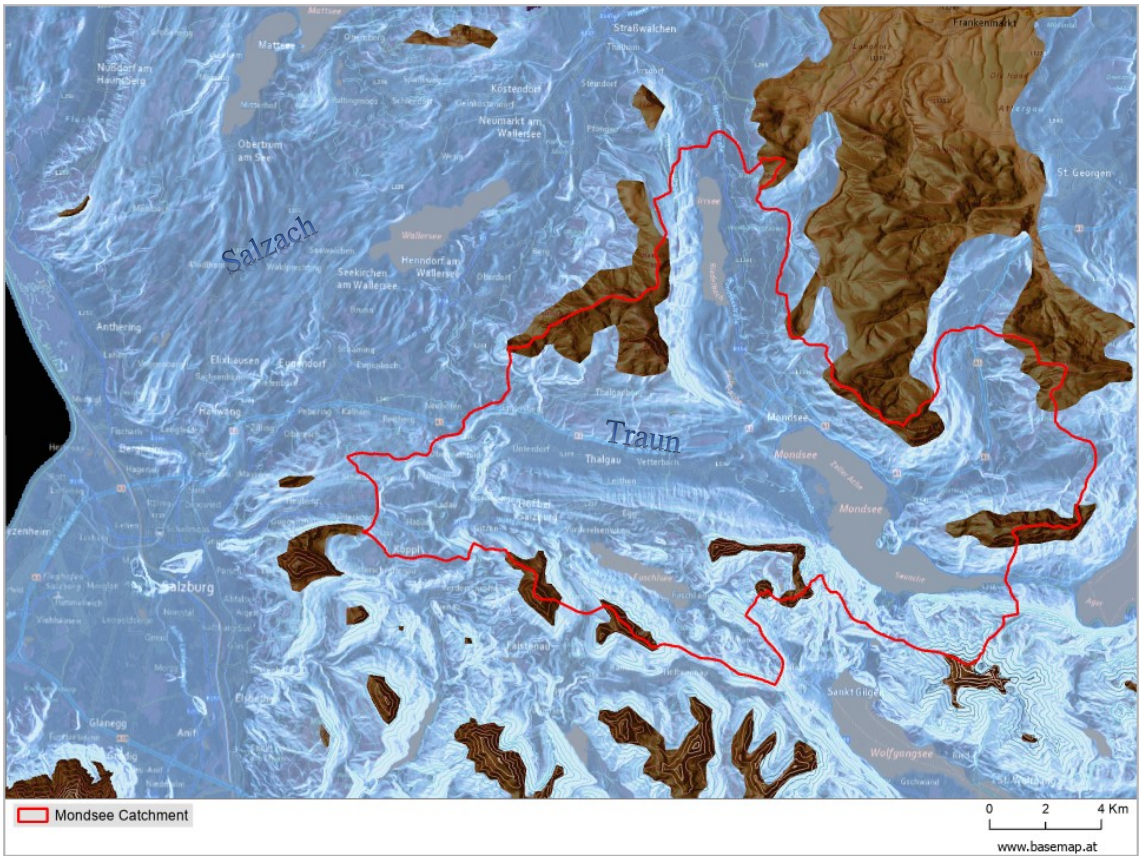

Figure 14: Riss glaciation reconstruction after Egger and Van Husen (2009) and Egger and Van Husen (2014) where the valleys of lakes Mondsee, Attersee, Irrsee, and Wolfgangsee were covered with ice.

The moraines of the Riss glaciation are embedded in the tongue basins of the Mindel glaciation (Kohl 1998), whereby Weinberger (in Del Negro 1969), distinguishes between two terminal moraines that are evident on the terrain. The dominant mountain range from the Riss glaciation, which even surpasses the Mindel moraines in height, starts on the west side of the Kogler mountain at about 660 m, moves - forming today's watershed - directly over the Ederbauer railway station to the north, then bends sharply West, reaches about 650-640 m asl before it breaks off at the Hainbach river, a headstream of the wide Mattig valley north of Straßwalchen (Kohl 1998). The terminal moraines of this glaciation east of Straßwalchen are widespread and well known; Weinberger (1955) also mentioned the broad walls near Ederbauer, Hochfeld, and Stockham-Bodenberg (Figure 15).

“The ice tongue of the Salzach Glacier in the Wallersee basin and that of the Traungletscher in the Irrsee basin were in contact in the saddle north of Sommerholz so

that the Irrsberg mountain rose north of it as the northernmost nunatak from the ice streams" (Weinberger 1955; Egger and Van Husen 2009) as well as "the mountains Schoibernberg and Kogler" (Weinberger 1955). In the Thalgau area, the ice flow of the Traun glacier, combined with that of the Salzach, was still almost 900 m high, probably due to the damming effect at the confluence; The ice masses penetrated the valley of the Fischbach between Große Plaike and Kolomansberg and filled it up to about this height, as evidenced by the ground moraine cover around Finkenschwandt (Egger and Van Husen 2009) (Figure 15).

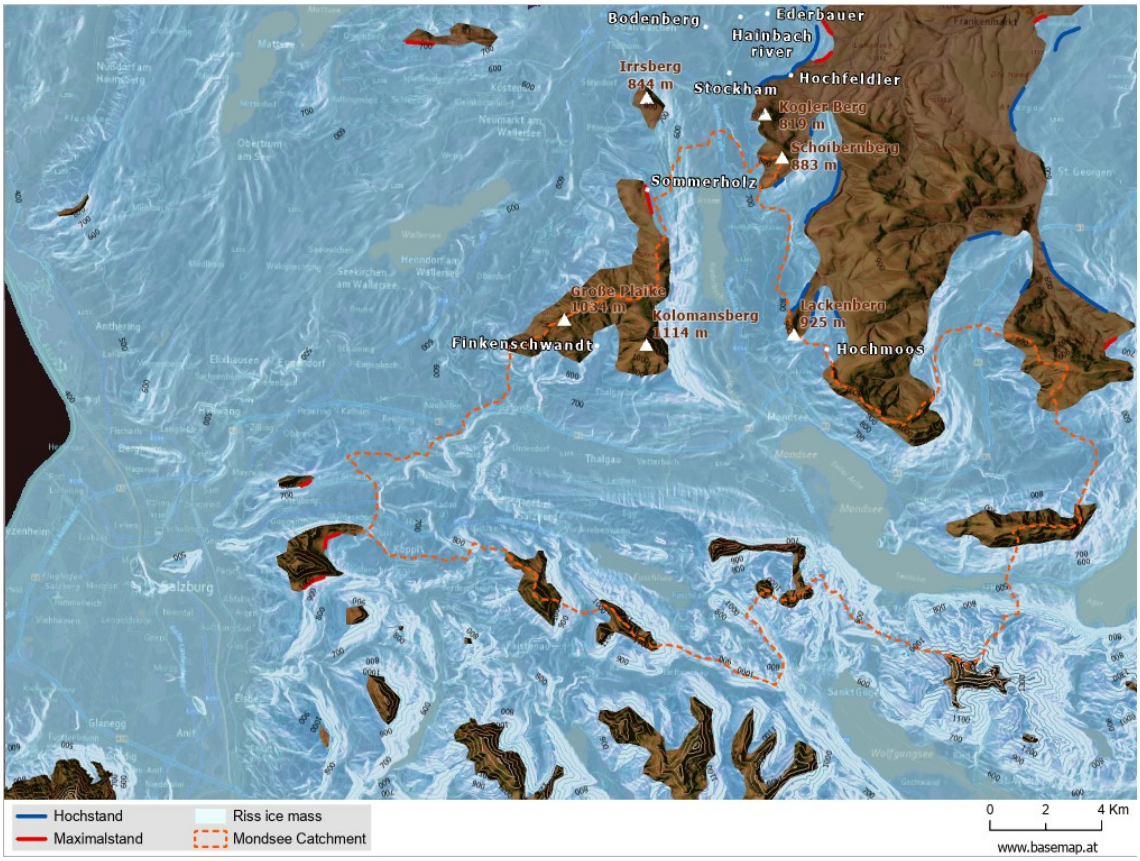

Figure 15: Riss ice reconstruction regarding the Irrsee lobe of the Traun glacier after Egger and Van Husen (2009; 2014).

Van Husen describes three lobes of the Traun glacier at the basin of Irrsee lake in his report (Van Husen 1986). The first flowed over the ridge at Hochmoos, the second over the broad trough near Haslau north of Lackenberg, and the third penetrated north of the Kogler mountain as far as Langholz – Obermühlham (N of Ederbauer, see Figure 15). This left behind a wide wall that can be traced from Hochfeldler via Matzlröth - Hechfeld to Unterreith (Figure 16) and is connected to a fluvioglacial deposit in the Vöckla valley. In front of it, there are remains of moraine walls near Obermühlham and north of the railway near Mazlröth, which probably belong to a somewhat larger extent level, but are not linked to a recognizable glaciofluvial deposit.

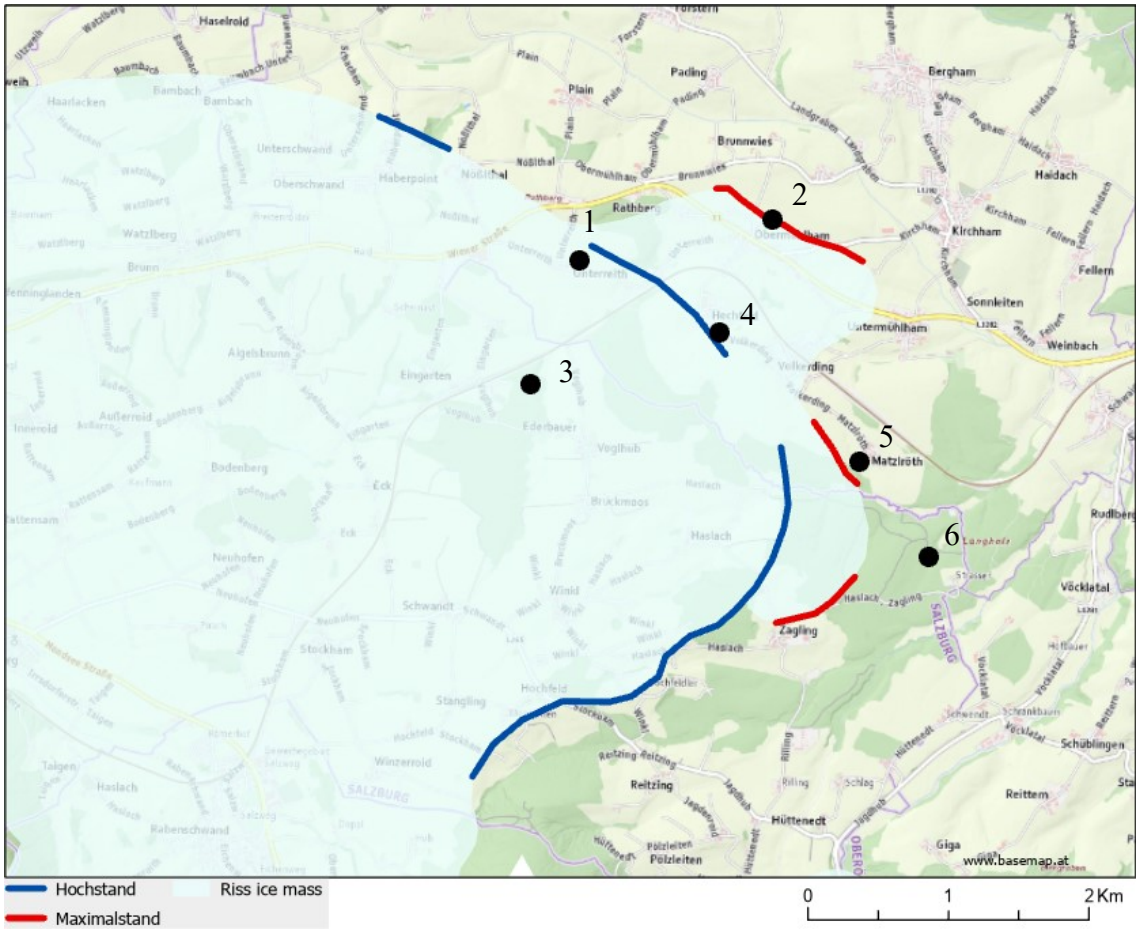

Figure 16: Northern lobe of the Traun glacier north of Irrsee, outside of the study area after Egger and Van Husen (2009; 2014). 1: Unterreith, 2: Obermühlham, 3: Ederbauer, 4: Hechfeld, 5: Maztlröth, 6: Langholz.

Van Husen (1986) continues his report on the ice tongue near Haslau deposited on the wide and curved moraine formed from Badlhof to Golau (Figure 17). The continuation of this wall is the walls formed from Breitenau to Vormoos. Equivalents to this moraine are the walls found at Oberholz to Jagdhub, which after a short break continue to the south. The smallest of the three ice tongues is formed above the saddle at Hochmoos. It reached about 400 m south of Vormoos and left behind the clear wall at Ebnat and equivalent sediments east of the Vöckla river.

The Riss glacial deposits at Winkl, between Koppl and Gaisberg, were also mapped in 1986. Meneweger (1993) mentions three preserved terminal moraines walls west of Koppl Moor and ESE of Nockstein (Figure 17). The highest is found at 875 m asl on the slope of Nockstein, and the other two emerge at 860 m and 830 m from the levelled and weathered ground moraines. Del Negro (1967) mentions only the two lowest. Meneweger (1993) also mentions the foothills east of Nockstein at 830 m asl where a long front of moraines remains, and at the north and south at 810 m a short one. On the eastern ridge at 970 m, he mentions Gosau erratics. Finally, he suggests that a maximum ice height of 880 m asl can be reconstructed over the terminal moraine walls.

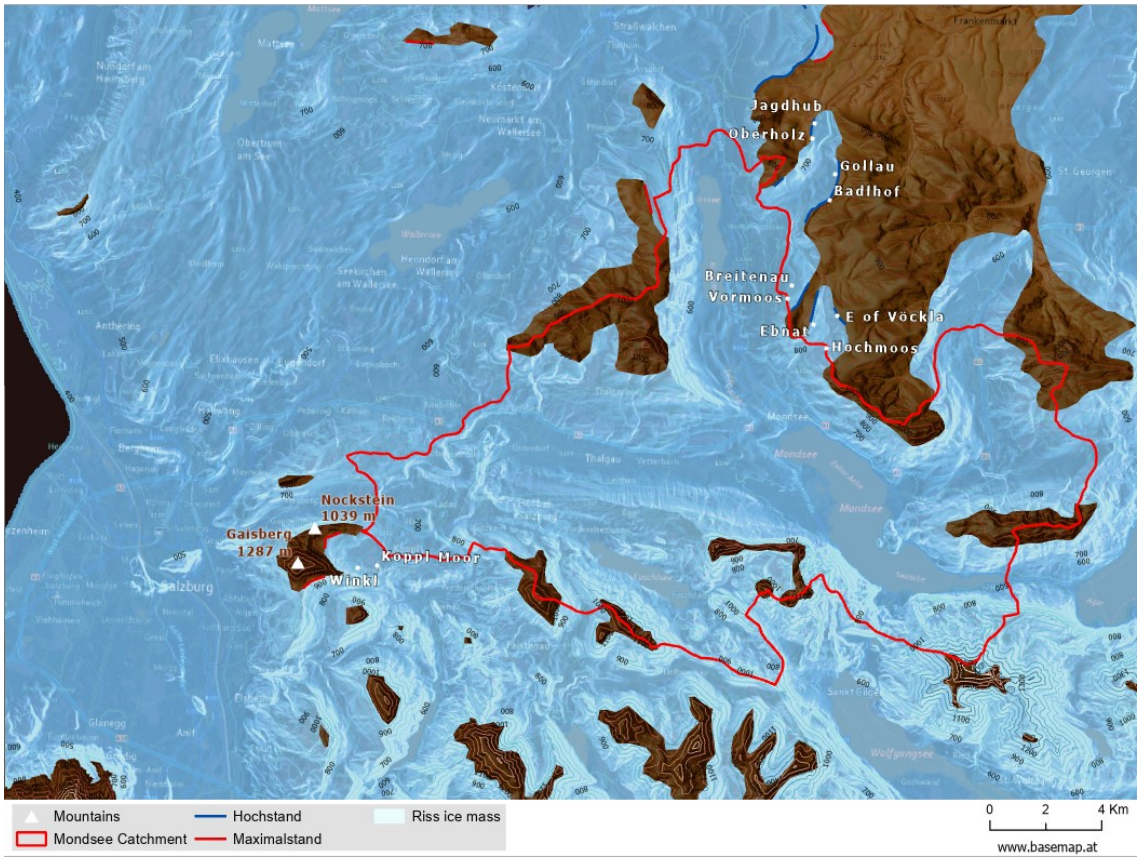

Figure 17: Riss ice reconstruction after Egger and Van Husen (2009; 2014).

"The fluvial gravel deposits were accumulated by braided rivers and were associated with the Riss terminal moraines of the Salzach glacier at Gilgenberg" (West of Mattighofen) (Weinberger 1955) and "of the Traun glacier at Lenzing (N of Lake Attersee), Schörfling (North end of Lake Attersee) and Gschwandt (East of Attersee, Traunsee)" (Egger and Van Husen 2007). To the interglacial "Gollinger See" (Penck and Brückner 1909; Weinberger 1955) various conglomerates, such as the Torrener Nagelfluh (molasse conglomerate) are found at the edge of the Salzburg basin near Golling, its type area, which is 25 km south of Salzburg.

After the end of the Riss Glaciation and the receding of the Traun glacier, a lake was formed from the melted ice that was probably much bigger and had a 40 m higher water level than today's lake Mondsee (Van Husen 2003) or 50 m according to Van Husen (2000) (Figure 18). This was first suggested after Klaus (1987). He investigated the sediments north of present lake Mondsee and considered them as the end progress from Riss to Würm. Later other pollen analyses on the Steinbach river's sediments revealed rapid reforestation after the end of the Riss glaciation (Van Husen 2003) similar to that after the Würm glaciation (Draxler 1977) supporting the previous beliefs. Recent investigations suggest a paleolake with a 540 m water level, 60 m higher than the present lake (Egger and Van Husen 2014). This could mean that lake Mondsee and Attersee were once one lake, however, according to Egger and Van Husen (2014) since the water level of Paleomondsee was higher than that of the Riss glacier outlet and higher than the terrace

of Ager river (490 m), the Riss end moraines at the northern end of Attersee could not serve as a dam. Therefore, they assume that the two lakes were separated by a barrier (most likely a kame terrace) from the Riss ice breaking-up period that was not pierced due to lack of strong outflow and probably because the erosive power of the small streams was nullified by the mudslides.

With the help of the 3D Analyst Toolbox of ArcGIS Pro Lake Paleomondsee was reconstructed and compared to the modern lake Mondsee (Figure 18). Up and to the right side of the image it can be observed that the water filled the area where the town Mondsee is today (Figure 18, 1) and then it can be assumed it did not advance further since its water level was at 540 m asl (Egger and Van Husen 2014). The dam between Mondsee and Attersee as described by Egger and Van Husen (2014) can also be seen in Figure 18, 2.

Figure 18: Paleomondsee (left) after Van Husen (2000), and Egger and Van Husen (2014) and present lake Mondsee (right). (1) Town Mondsee, (2) Dam between Mondsee and Attersee (dashed line), (3) Schafberg, (4) Drachenwand.

2.1.3 Mindel Glaciation

Weinberger (1955), Del Negro (1969), and Kohl (1997) mentioned Mindel moraines as terminal moraines with reference to "the area between the Salzach glacier in the west and the Krems glacier in the East" (Weinberger 1955; Del Negro 1969; Kohl 1997; Egger and Van Husen 2003). During this glaciation, the catchment is again filled with ice from the Salzach glacier from the west and the Traun glacier from the east. The terminal moraines of this glaciation are noticeably more powerful, closed walls that indicate a longer-lasting, stable end position with small fluctuations (Penck and Brückner 1909; Weinberger 1950; Del Negro 1967; Grimm et al. 1979).

Originating in the Hohe Tauern, Central Alps, the Salzach Glacier covers an area of 7.510 km^2 (Brückner 1886) and reaches its maximum extent during the Mindel glaciation (Weinberger 1955). The deposits of the Piedmont glacier tongue east of the Salzach that are attributed to the Mindel Glaciation (Weinberger 1955) indicate a spread of ice up to the southern edge of the Kobernaußer Forest, which must have completely covered the area, N of the Mondsee catchment (Figure 21).

Figure 19: Reconstruction of the Mindel maximum glaciation modified after Egger and Van Husen (2009; 2014), Weinberger (1955).

From the limestone Alps (southern part of the area) only Gaisberg, Schwarzenberg, and Schober protruded as nunataks, whereas from the Flysch zone (northern part) only Kolomansberg, and probably Tannberg and Irrsberg (Egger and Van Husen 2009) (Figure 19). In his geologic map, Weinberger (1955) presents the south side of mountain

Tannberg covered with Riss terminal moraines whereas the north-east side is covered with Mindel terminal moraines. This helped with the ice reconstruction of Mindel (Figure 21).

The three tongues of the Traungletscher (Irrsee, Attersee, Traunsee) each formed their own lobes, which in the west reached the southern edge of the Kobernaußer forest (Weinberger 1955; Del Negro 1969). Terminal moraines are also found at Weißenkirchen, Pfaffing, and Hehenberg (Weinberger 1955; Del Negro 1969; Egger and Van Husen 2007). These experts mentioned other sightings at Forstern, Laakirchen, and Rabesberg but these are well outside of the catchment area and the scope of this study. Only a generalized representation is presented here (Figure 21).

Egger and Van Husen (2009) describe two circular erosion formations with a diameter of approx. 3 m and approx. 5 m and a depth of around 4-6 m just below the summit of the isolated mountain Nockstein, N of Gaisberg, which rises to 1.042 m. They describe them as kettle holes, which could only be created on summits as glacier mills under ice cover from meltwater. According to the existing height marks (terminal moraines), the summit area was not covered by ice, neither during the Riss nor the Würm glaciations, but only at the time of the most intensive glaciation, the Mindel glaciation (Weinberger 1955). Thus, the formation of the kettle holes can be assumed that it originated during Mindel. According to Egger and Van Husen (2009) these kolks indicate that the ice stream was at least 1.050 – 1.100 m at that time for the meltwater to create this landform (Figure 20).

Figure 20: Photo from inside the kolk at the summit area of Nockstein.

Since there are no other images regarding the Ice Reconstruction of the Mindel glaciation in the study area and its surroundings, Figure 19 and Figure 21 were created manually with the various editing tools of ArcGIS Pro and were modified after Egger and Van Husen (2009), Weinberger (1955), after their observations and findings, as well as after Meneweger (1993), Egger and Van Husen (2014), and Kohl (1998). The reason why this glaciation, and its predecessor, Günz, have not been extensively examined in this study

like the previous ones is that they extend further outside the study area and the sediments and landforms they left behind in the study area were covered by the sediments of the younger glaciations, Riss and Würm. Therefore, their documentation is related more to the terminus areas of the glaciers and not their main body that flowed in the Mondsee catchment. Furthermore, the distinction between Mindel and Günz is also difficult since their advance was approximately the same with a few exceptions where Günz terminal moraines exceeded those of Mindel.

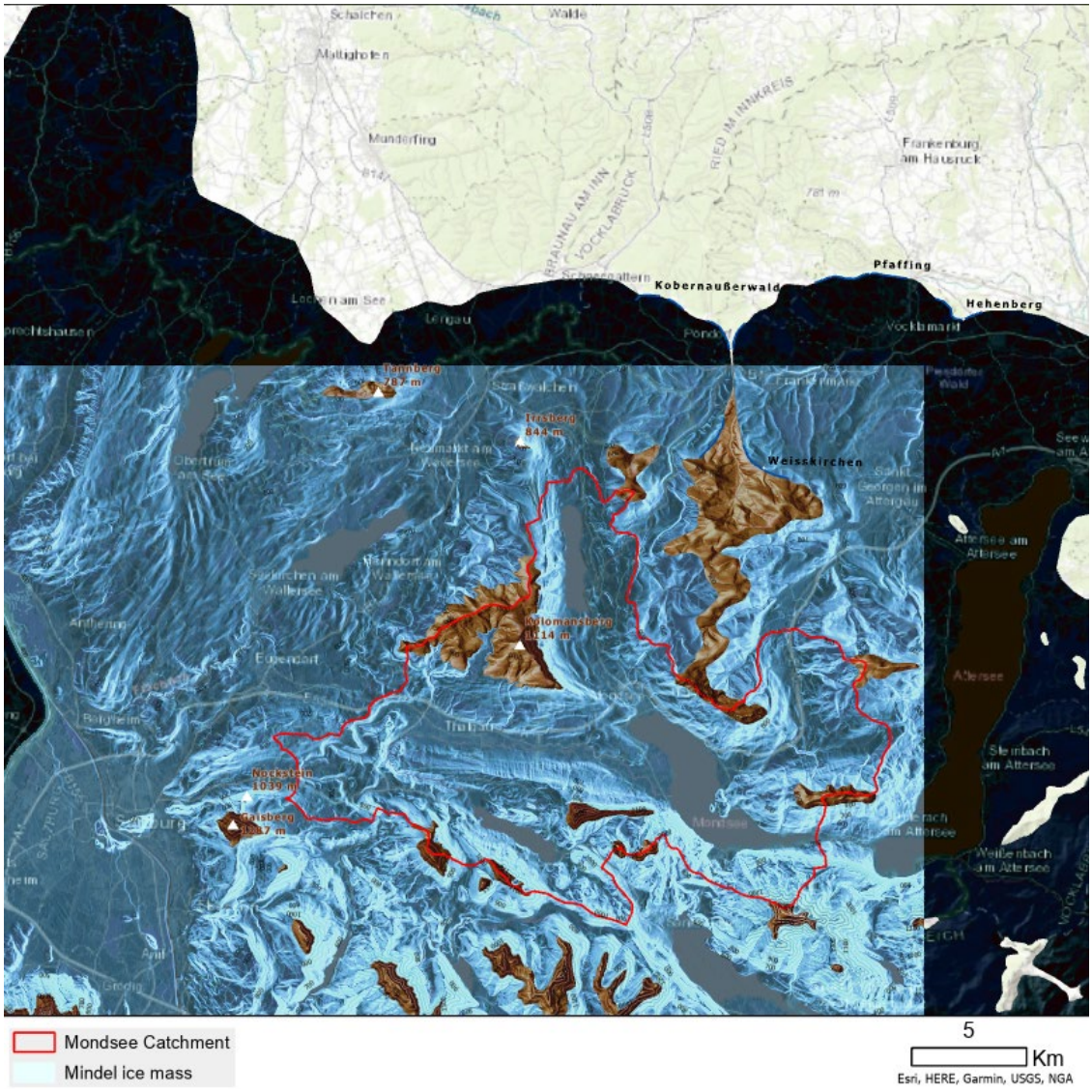

Figure 21: Mindel ice reconstruction after Egger and Van Husen (2009), Weinberger (1955), Meneweger (1993), Egger and Van Husen (2014), and Kohl (1998).

2.1.4 Günz Glaciation

Günz is the first of the Alpine Pleistocene glaciations and reaches farther outside of the study area. This first verifiable glacial expansion transformed the landscape and the water network by eroding and transporting loose sediments from the northern edge of the Alps to the foreland (Egger and Van Husen 2014). Deposits associated with this first advance were found only along the Vöckla river (Sperl 1984) north of the study area and it cannot be said with certainty if this advance took place in the Günz glaciation (MIS 16) (Van Husen and Reitner 2011) or if it originated in an early oscillation of the Mindel glaciation (MIS 12) (Egger and Van Husen 2014).

As with the Mindel, so is Günz glaciation not covered in depth in this study, as it extends further outside the boundaries of the study area. The ice reconstruction (Figure 22) was created after Egger and Van Husen (2009), Weinberger (1955), Meneweger (1993), Egger and Van Husen (2014), and Kohl (1998).

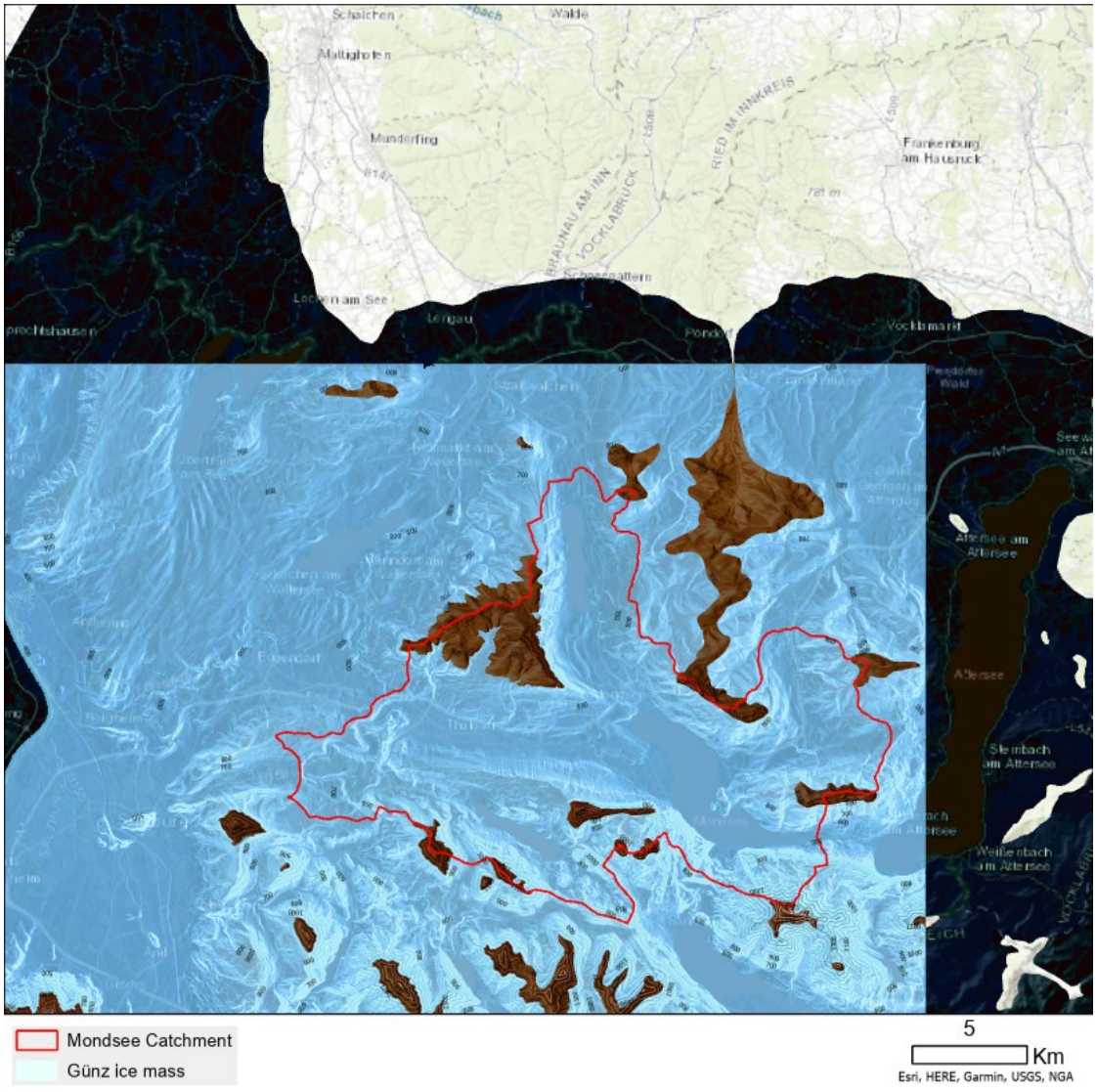

Figure 22: Günz ice reconstruction after Egger and Van Husen (2009), Weinberger (1955), Meneweger (1993), Egger and Van Husen (2014), and Kohl (1998).

Unmistakably, Günz moraines are found at the northern part of Siedelberg mountain, west of Mattighofen and are associated with the Älterer Deckenschotter (ÄD) sheet Weinberger (1950). On the easternmost branch of the Traungletscher, Günz moraines are well-preserved N of the Traunsee basin near Berg on the motorway between Vorchdorf and Steyrermühl, east of Laudach (Kohl 2001a; Egger et al. 2018). Kohl (1958) interpreted the end moraines around Sattledt, which merge into the widespread older sheet gravel of the Traun-Enns Platte, as the end position of the Günz-glaciation Krems glacier. Furthermore, outside the state of Salzburg, near Frankenmarkt, there are advanced gravel and ground moraines of the Günz glaciation (Sperl 1984).

2.2 Data sources and software

The western part of the study area is in the Federal State of Salzburg, which offers Digital Terrain Models (DTM) derived from Airborne Laser Scanning (ALS) measurements with a resolution of one meter for each municipality online (Land Salzburg). The eastern part of the area is in the federal state of Upper Austria, which offers the 0,5-meter resolution DTMs for each municipality, also derived from ALS measurements, online in xyz format (Land Oberösterreich).

The ArcGIS Pro software from ESRI offers a variety of tools that helped with the preprocessing of the data as well as with the analysis. The DTMs were assembled into a mosaic and merged into a new raster of 1m resolution (Figure 23). This raster was used consecutively to deduce a contour layer and a hill shade layer. These layers were crucial to identifying glacier landforms and assisting with the geomorphologic analysis of the study. All figures and maps in this study were created in ArcGIS Pro.

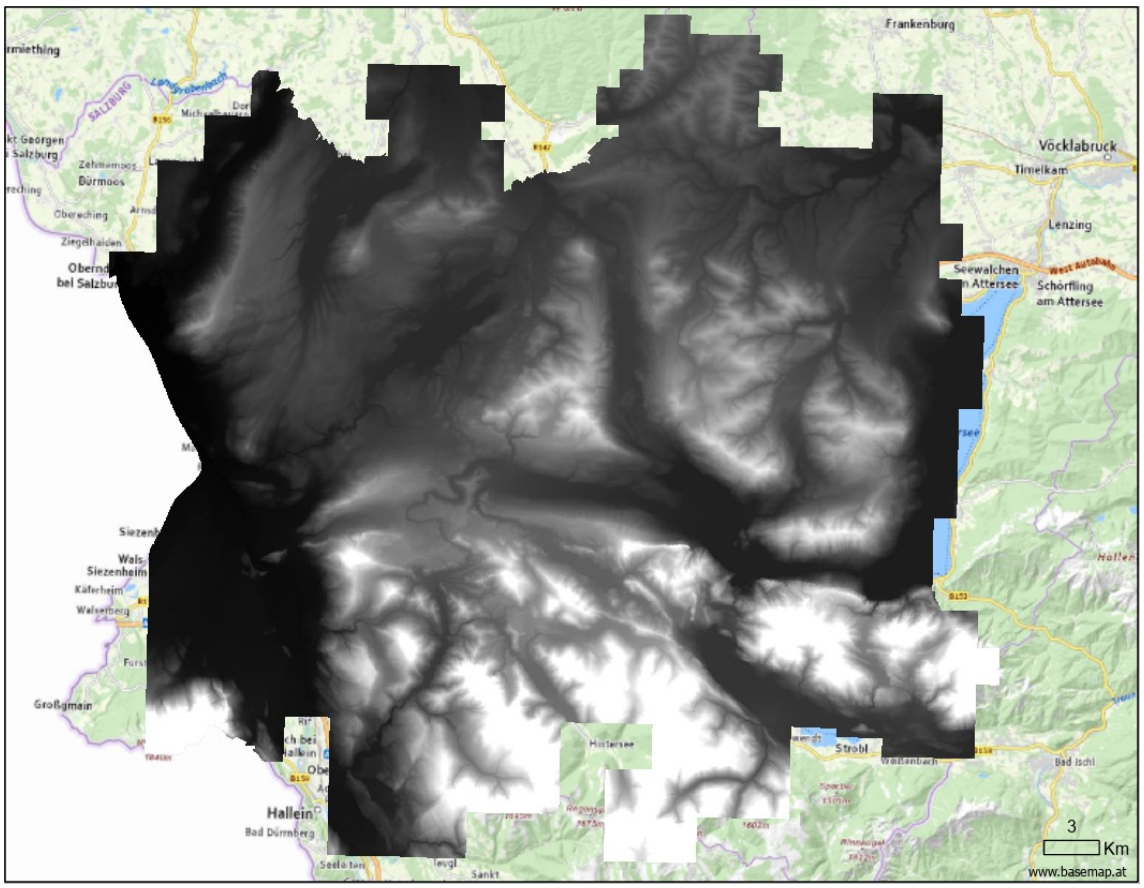

Figure 23: Mosaic raster combined from the point data of each municipality of the cities Salzburg and Upper Austria (Oberösterreich). The raster was then clipped, resampled, and projected in UTM Zone 33N.

Another fundamental geospatial data source was scientific literature written by local experts in the native language covering the quaternary glaciation of the study area and its surroundings. This includes published and non-published scientific papers as well as reports, lectures, and articles (Figure 24). Experts describe geomorphological features

(e.g., drumlins, moraines, etc.) and their localities in the field, which are digitized as points, lines, or polygons. Additionally, maps in JPEG format found in the literature were orthorectified and used to manually delineate features and create new layers and maps.

Most of the sightings found in the literature were "translated" as points or lines in reference to the nearest place they were sighted by the authors. In this regard, the coordinates of these locations were recovered from local topographic maps, such as the basemap provided by Open Government Data of Austrian administrations (https://basemap.at/), and transferred as point features in ArcGIS Pro. The moraine walls were translated as line features deducted from the terrain model of the area and the contour lines.

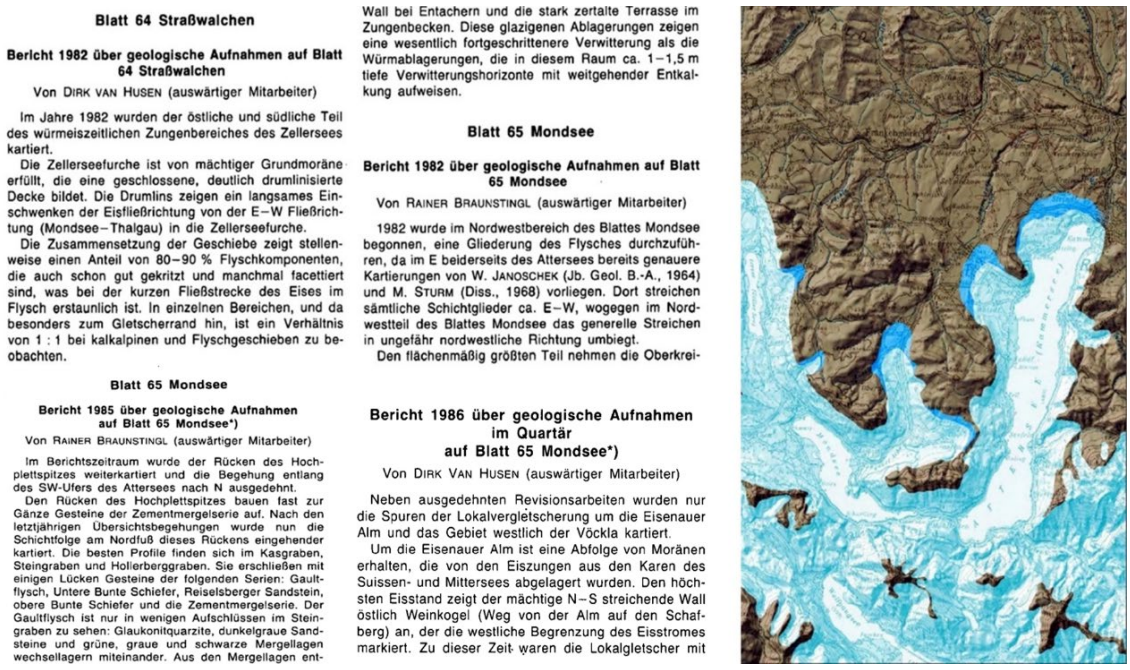

Blatt 64 Straßwalchen

Bericht 1982 über geologische Aufnahmen auf Blatt 64 Straßwalchen

Von DIRK VAN HUSEN (auswärtiger Mitarbeiter)

Im Jahre 1982 wurden der östliche und südliche Teil des würmeiszeitlichen Zungenbereiches des Zellersees kartiert.

Die Zellerseefurche ist von mächtiger Grundmoräne erfüllt, die eine geschlossene, deutlich drumlinisierte Decke bildet. Die Drumlins zeigen ein langsames Einschwenken der Eisfließrichtung von der E–W Fließrichtung (Mondsee–Thalgau) in die Zellerseefurche.

Die Zusammensetzung der Geschiebe zeigt stellenweise einen Anteil von 80–90 % Flyschkomponenten, die auch schon gut gekritzt und manchmal facettiert sind, was bei der kurzen Fließstrecke des Eises im Flysch erstaunlich ist. In einzelnen Bereichen, und da besonders zum Gletscherrand hin, ist ein Verhältnis von 1 : 1 bei kalkalpinen und Flyschgeschieben zu beobachten.

Blatt 65 Mondsee

Bericht 1985 über geologische Aufnahmen auf Blatt 65 Mondsee*)

Von RAINER BRAUNSTINGL (auswärtiger Mitarbeiter)

Im Berichtszeitraum wurde der Rücken des Hochplettspitzes weiterkartiert und die Begehung entlang des SW-Ufers des Attersees nach N ausgedehnt.

Den Rücken des Hochplettspitzes bauen fast zur Gänze Gesteine der Zementmergelserie auf. Nach den letztjährigen Übersichtsbegehungen wurde nun die Schichtfolge am Nordfuß dieses Rückens eingehender kartiert. Die besten Profile finden sich im Kasgraben, Steingraben und Hollerberggraben. Sie erschließen mit einigen Lücken Gesteine der folgenden Serien: Gaultflysch, Untere Bunte Schiefer, Reiselsberger Sandstein, obere Bunte Schiefer und die Zementmergelserie. Der Gaultflysch ist nur in wenigen Aufschlüssen im Steingraben zu sehen: Glaukonitquarzite, dunkelgraue Sandsteine und grüne, graue und schwarze Mergellagen wechsellagern miteinander. Aus den Mergellagen entWall bei Entachern und die stark zerfalte Terrasse im Zungenbecken. Diese glazigenen Ablagerungen zeigen eine wesentlich fortgeschrittenere Verwitterung als die Würmablagerungen, die in diesem Raum ca. 1–1,5 m tiefe Verwitterungshorizonte mit weitgehender Entkalkung aufweisen.

Blatt 65 Mondsee

Bericht 1982 über geologische Aufnahmen auf Blatt 65 Mondsee

Von RAINER BRAUNSTINGL (auswärtiger Mitarbeiter)

1982 wurde im Nordwestbereich des Blattes Mondsee begonnen, eine Gliederung des Flysches durchzuführen, da im E beiderseits des Attersees bereits genauere Kartierungen von W. JANOSCHEK (Jb. Geol. B.-A., 1964) und M. STURM (Diss., 1968) vorliegen. Dort streichen sämtliche Schichtglieder ca. E–W, wogegen im Nordwestteil des Blattes Mondsee das generelle Streichen in ungefähr nordwestliche Richtung umbiegt.

Den flächenmäßig größten Teil nehmen die Oberkrei-

Bericht 1986 über geologische Aufnahmen im Quartär auf Blatt 65 Mondsee*)

Von DIRK VAN HUSEN (auswärtiger Mitarbeiter)

Neben ausgedehnten Revisionsarbeiten wurden nur die Spuren der Lokalvergletscherung um die Eisenauer Alm und das Gebiet westlich der Vöckla kartiert.

Um die Eisenauer Alm ist eine Abfolge von Moränen erhalten, die von den Eiszungen aus den Karen des Suissen- und Mittersees abgelagert wurden. Den höchsten Eisstand zeigt der mächtige N–S streichende Wall östlich Weinkogel (Weg von der Alm auf den Schafberg) an, der die westliche Begrenzung des Eisstromes markiert. Zu dieser Zeit waren die Lokalgletscher mit

Figure 24: On the left there are reports on the geological surveys of the Straßwalchen and Mondsee areas from different years and on the right a map representing the reconstructed ice sheet covering the study area during the Würm glaciation after Egger and Van Husen 2014.

2.3 Methodology

2.3.1 Geomorphometry

Geomorphological maps can be derived either from field "mapping and digitization of features through field surveys, and topographic data, or via orthoimagery, and remote sensing" (Dent and Young 1981; Pain 1985; Bocco et al. 2001; Lambiel et al. 2016). According to Pike et al. (2009), "geomorphometry is the science of quantitative land-surface analysis and its fundamental operation is to extract parameters and objects from DEMs". Basic parameters include the slope gradient, aspect, and curvature to describe the local morphology (Figure 25). Hydrological or flow-accumulation parameters such as indices of erosion or mass movement reflect the potential movement of material over the land surface.

In the last decades, the extraction of these parameters is enhanced by quantitative methods to classify landforms like supervised and unsupervised techniques (Brown et al. 1998; Prima et al. 2006; Dragut and Blaschke 2006; Jones et al. 2007). Supervised classification uses training data/classes assigned by an expert whereas unsupervised classification assigns unlabelled data to classes without the need for human intervention.

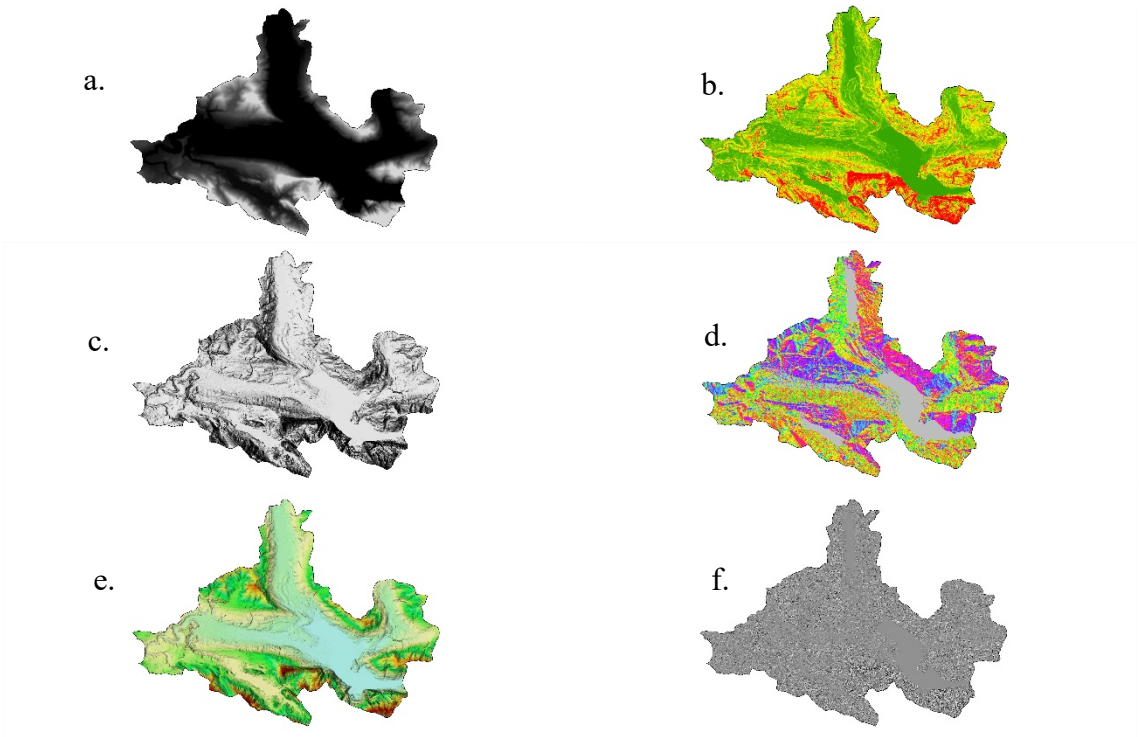

Figure 25: Mondsee Catchment (a) Digital Elevation Model (DEM), (b) Slope Gradient, (c) Hillshade, (d) Aspect, (e) Shaded Relief, (f) Curvature.

The curvature layer at a smaller scale is filled with noise and does not present the desired outcome due to generalization. (Figure 26). This output shows the surface as a plane fitted through a cell and its eight surrounding neighbors.

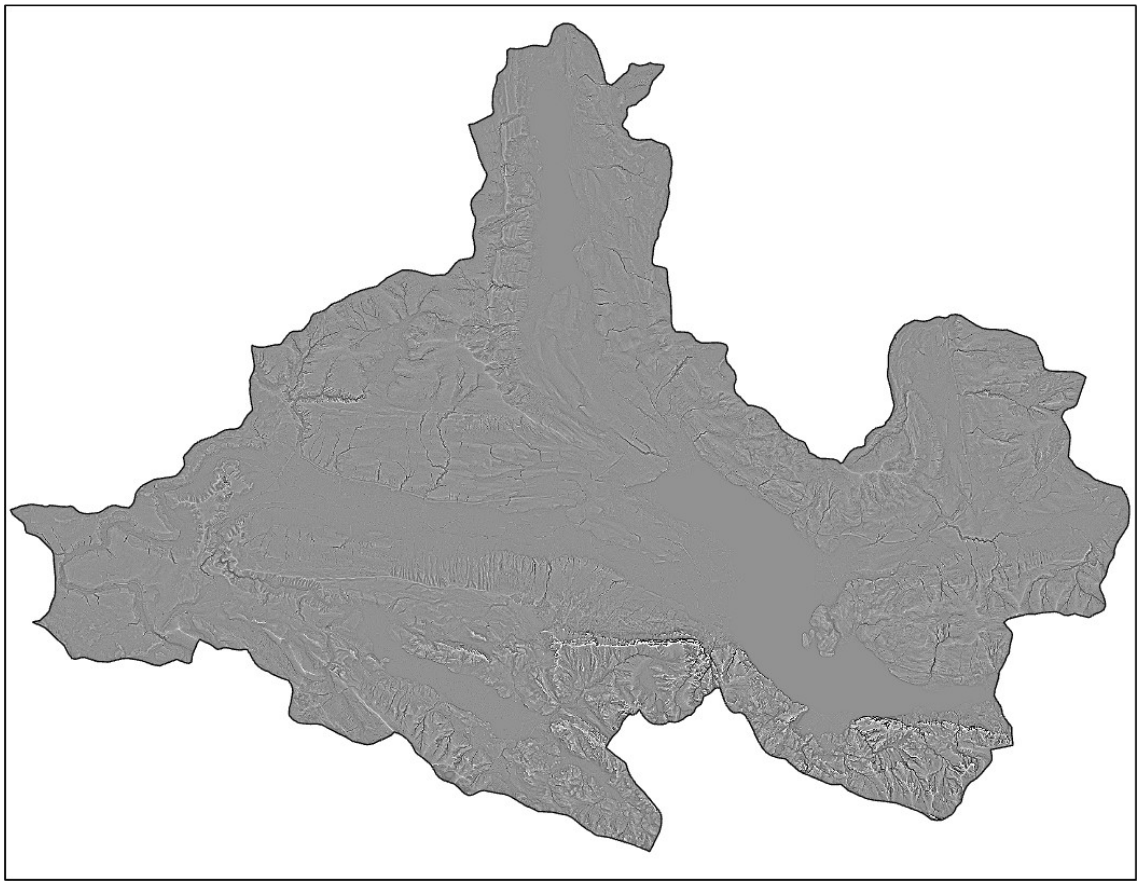

Figure 26: Standard Curvature raster of the Study Area.

The geomorphometric parameters were utilized in conjunction with automated classification to extract a geomorphologic map. The Geologic maps of Sheet 64 of Strasswalchen (Egger and Van Husen 2003) and Sheet 65 of Mondsee (Van Husen 1989b) were used as input to classify the various sediments and rocks of the area. The maps were initially imported in ArcGIS Pro, Georectified, and mosaicked together to form one map (Figure 27).

Both object-based, and pixel-based supervised classification was examined. An increasing trend in dissatisfaction toward pixel-based analysis and a general turn toward object-based analysis (OBIA) and image segmentation is observed (Burnett and Blaschke 2003; Blaschke 2010). Blaschke and Strobl (2001) raised the question, "*what is wrong with pixels?*" addressing this topic and suggested concentrating on the spatial patterns of the pixels and not the statistical analysis of single pixels. Each real-life object has a specific shape and size, its geometry, and has a spatial relation to its neighbour, and extracting this information can help answer scientific questions.

With object analysis, the result is usually more homogenous, whereas with pixel analysis is fragmented. Both analyses were used to extract the classes that were optimized in another step with the help of the on-screen editing tools of ArcGIS Pro. The support vector machine (SVM) was used as a classifier for both analyses. This classifier "is a computer algorithm that learns by example to assign labels to objects" (Boser et al. 1992)

and it is widely used together with GIS like, for example, in landslide susceptibility (Tehrany et al. 2014; 2015). This classifier is great for large images and is less affected by noise or by an unbalanced number in the samples for each training class.

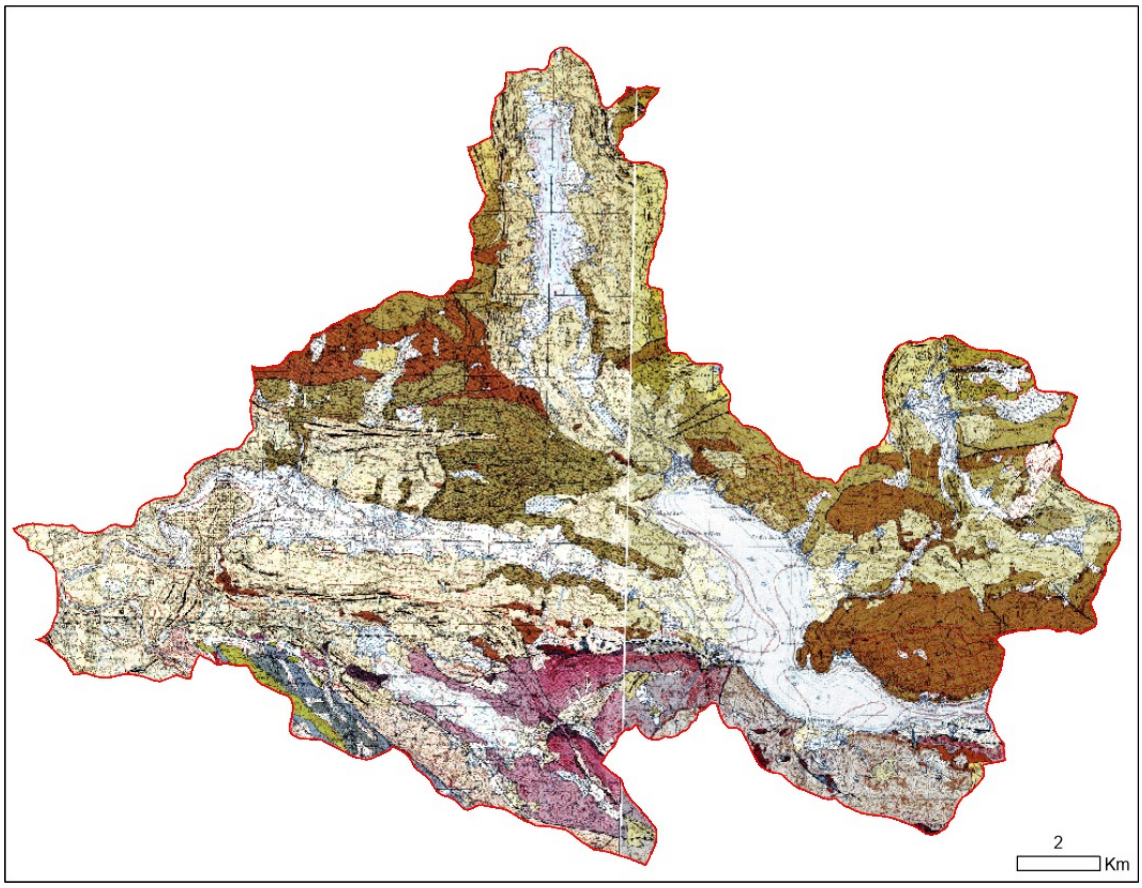

Figure 27: Geological Maps of Sheet 64 Strasswalchen (Egger and Van Husen 2003) and Sheet 65 Mondsee (Van Husen 1989b) mosaicked into one map.

As shown in Figure 27, the area is characterized by a variety of landforms, sediments, and rocks and is already not homogenous. Therefore, only the most prominent classes were sampled, whereas different classes were merged into one class for simplicity, for example, ground, and terminal moraines either of the Würm or Riss glaciation were sampled as one class and used as training data for the model. Ultimately, 500 assessment points were created and used to compute a confusion matrix that lists the errors for each class and derives a kappa index to assess the overall classification accuracy.

The image analysis was conducted via the Image Classification Wizard tool and ultimately, the geomorphological map was extracted from the OBIA analysis results and on-screen editing in combination with a variety of labelling options available in ArcGIS Pro.

2.3.2 Orthorectification

Images from scientific papers were imported and used for the analysis. Each image was georeferenced by projecting and assigning coordinates and orthorectified by modifying the geometry with GCPs (Ground Control Points) and 2nd order polynomial transformation in ESRI's ArcGIS Pro 2.9.0 software (Figure 28). The transformation shifts, scales, and rotates the images with the following equations.

$$x^1 = Ax + By + C$$
$$y^1 = Dx + Ey + F$$

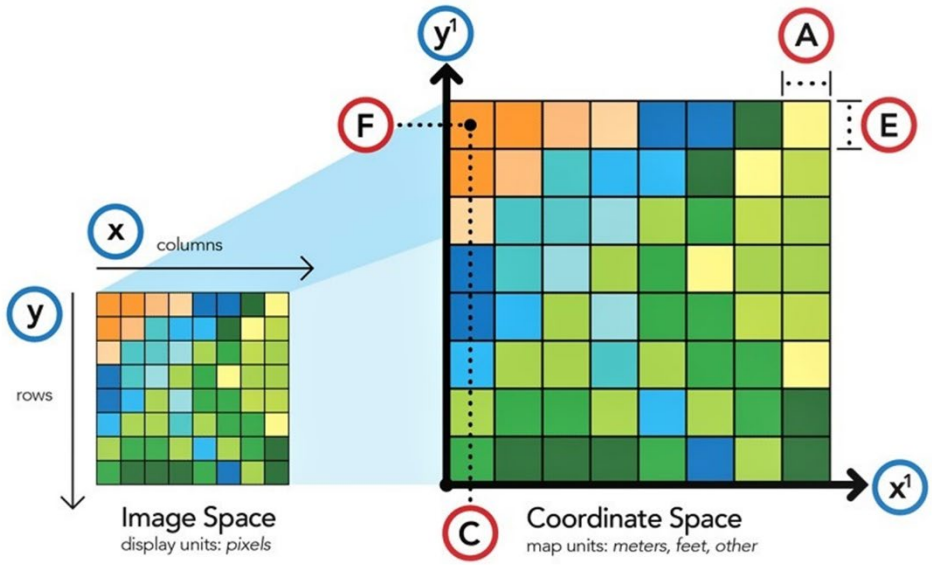

x : column count in image space
y : row count in image space
x^1 : horizontal value in coordinate space
y^1 : vertical value in coordinate space

A : width of the the cell in map units
B : a rotation term
C : x^1 value of the center of the upper-left cell
D : a rotation term
E : negative height of the cell in map units
F : y^1 value of the center of the upper-left cell

Figure 28: ESRI's Documentation on Georeferencing (Overview of Georeferencing)

Leys and Werritty (1999) analyzed "historical planform change using scanned maps" and suggested that "GCPs should be widely distributed across the image to provide a stable warp". Campbell and Wynne (2011) suggested that "GCPs should be dispersed throughout the image with good coverage near the edges".

For the orthorectification in this study, the control points were mainly selected from distinctive features such as road intersections (motorways and major roads), rock outcrops, and mountaintops that could be identified both in the source and reference image.

2.3.3 Interpolation

Interpolation is used to "predict unknown values from data such as elevation". This method premises Tobler's law of geography that objects close to each other share similar characteristics and are more related than objects that are further away (Tobler 1970). Although the theory holds up, in practice one must also consider the accuracy issues that arise as well as the impact of an inaccurate layer on the analysis. Gold (1989) explains the spatial adjacency issues while performing the weighted average method or the local polynomial technique. Some studies focused on "spatial data uncertainty" (Goodchild and Gopal 1989; Goodchild 1993; Hunter et al. 1995) while other studies focused on the comparative analysis of interpolation methods (Weng 2006; Mitas and Mitasova 1999; P.V. Arun 2013).

Zimmerman et al. (1999) showed that "the Kriging method provided a better estimation of altitude than the Inverse Distance Weight (IDW) method". However other studies (Weber and Englund 1992; Declercq 1996; Aguilar et al. 2005) showed that "the IDW method was as accurate as Kriging`s or even better". For this study both IDW and Kriging were used on the scattered elevation data gathered from literature to show the reader the difference between the two techniques and evaluate their accuracy but without focusing on the latter because it is not in the scope of this work.

The theoretical premise of the Kriging method was developed by French mathematician Georges Matheron in the 1960s (Matheron 1960, 1963). The method weights the surrounding measured values and predicts the value of an unmeasured location. The IDW method is similar to Kriging in this part. Both methods use the following formula in ArcGIS Pro (ArcGIS Pro documentation on Kriging):

$$\hat{Z}(s_o) = \sum_{i=1}^{N} \lambda_i Z(s_i)$$

Where: $Z(s_i)$ = the measured value at the ith location

λ_i = an unknown weight for the measured value at the ith location

s_0 = the prediction location

N = the number of measured values

Whereas the weights in IDW depend only on the distance to the prediction location, the Kriging method also examines the spatial distribution of the measured points. "In ordinary kriging, the weight, λ_i, depends on a fitted model to the measured points, the distance to the prediction location, and the spatial relationships among the measured values around the prediction location".

Both techniques were used to deduce the ice height using the Geostatistical Wizard of ArcGIS Pro. The output layer was exported as a raster layer and clipped with the ice masses of the Würm glaciation. The data used in the interpolation were extracted from scientific papers as information regarding the Würm glaciation and manually placed as 3D points on the map in ArcGIS Pro (Table 2). Some of the points were deduced from the orthorectified images after Egger and Van Husen (2009; 2014) that portrayed the ice reconstruction of the region to increase the number of data points in order to obtain satisfying results from the interpolation.

Finally, both raster surfaces created from IDW, and Kriging were further analyzed with the Surface Volume tool of ArcGIS Pro which calculates the area volume between a surface and a reference plane.

2.3.4 Story Map

Parallel with the recent accelerated advance of GIS, Story Maps have also seen rapid development and are being used as an informational tool in many fields, such as in Geomorphology (Antoniou et al. 2018b), in Geology (Antoniou et al. 2018a) or an educational tool in schools (Berendsen et al. 2018; Groshans et al. 2019). Baker (2015) emphasizes “the effectiveness of web GIS and mapping as a tool for improving student learning”.

A Story Map is not just a static map, but rather a way of communicating information and knowledge through videos, images, graphs, and text. Graves (2015) notes “that users are more likely to engage in a story that sustains their interest with a variety of text, maps, graphs, video, and audio clips to maximize the story’s overall content”. In addition to being interactive, the maps can be combined with GPS (Global Positioning System) so that the users can use their current location. This feature is very useful because it can provide the user with the ability to visualize the study site and its surroundings in 2D and 3D while in the field.

In this work after uploading all necessary layers in ArcGIS Online, an interactive and informative ArcGIS StoryMap was created. Web maps, images, and videos including narrative text were used. The web maps present the results of the analysis, the geomorphological map, and vector layers of points, lines, and polygons revealing the locations of glacial features in the catchment area of Lake Mondsee. This Story Map presents a holistic view of the area and its surroundings while informing the user about its origin and present form. All web maps allow the user to display his current location, thus providing him with an essential tool for field work.

3 Results

3.1 Geomorphometry

Using the methods described in chapter 2.3.1 the geomorphological map of Lake Mondsee`s catchment area was extracted (Figure 29). The map shows the area`s present form and how it is classified in its various formations. It is categorized into Quaternary formations, the two glaciations (Würm and Riss), and rock formations: Flysch, a succession of sedimentary rock strata covering the northern part of the area, and the Northern Limestone Alps, composed of limestone and dolomite, covering the southern part).

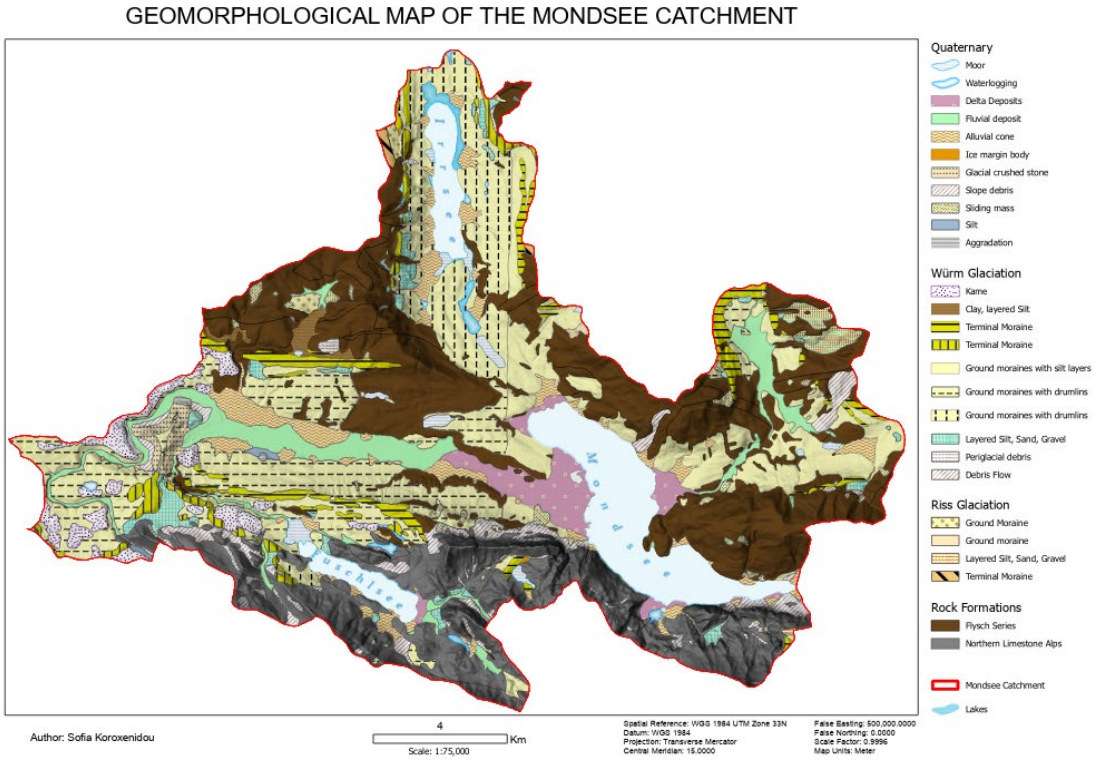

Figure 29: Geomorphological map of the Mondsee catchment after Egger and Van Husen (2003) and Van Husen (1989b).

3.2 Orthorectification

The following examples (Figure 30) are two images recovered from Egger and Van Husen (2009) and Egger and Van Husen (2014) that are neither georeferenced nor rectified and show the reconstructed ice of the Würm glaciation for the western and eastern part of the study area respectively. After the georectification, the images were analyzed further (Figure 31). The same procedure applied for the Riss (Figure 32 & Figure 33) and Mindel Glaciations (Figure 34 & Figure 35).

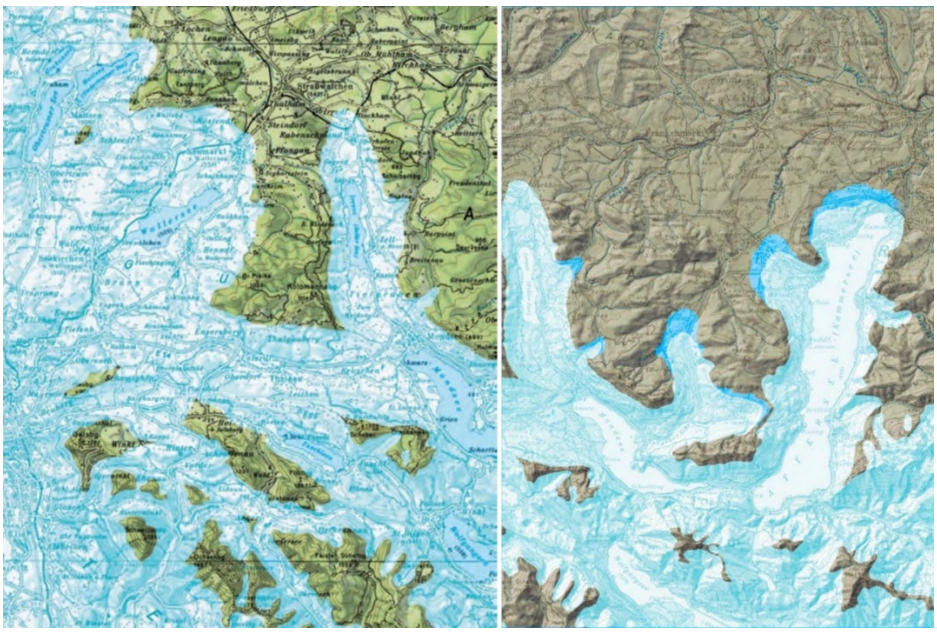

Figure 30: Non Georectified images from Egger and Van Husen (2009) (left) and from Egger and Van Husen (2014) (right).

Figure 31: Georectified images showing the Würm Glaciation: the left from Egger and Van Husen (2009) and the right from Egger and Van Husen (2014).

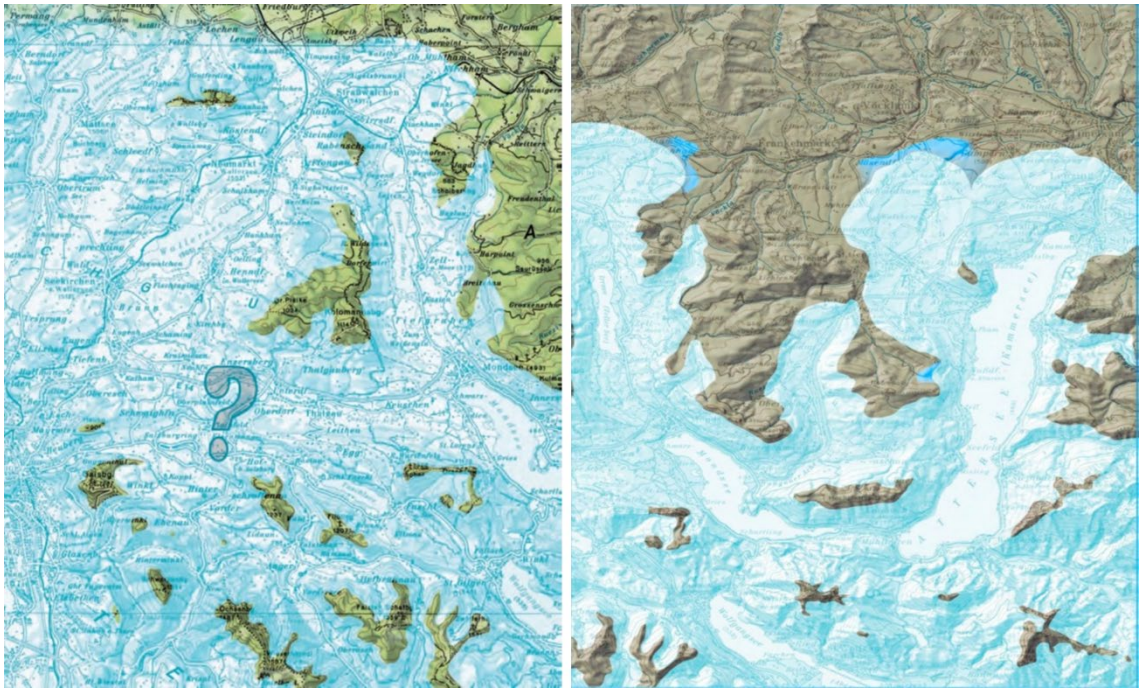

Figure 32: Non Georectified images showing the Riss glaciation ice reconstruction. Left: Image taken from Egger and Van Husen (2009) covering the western part of the study area. Right: Image taken from Egger and Van Husen (2014) covering the eastern part of the area.

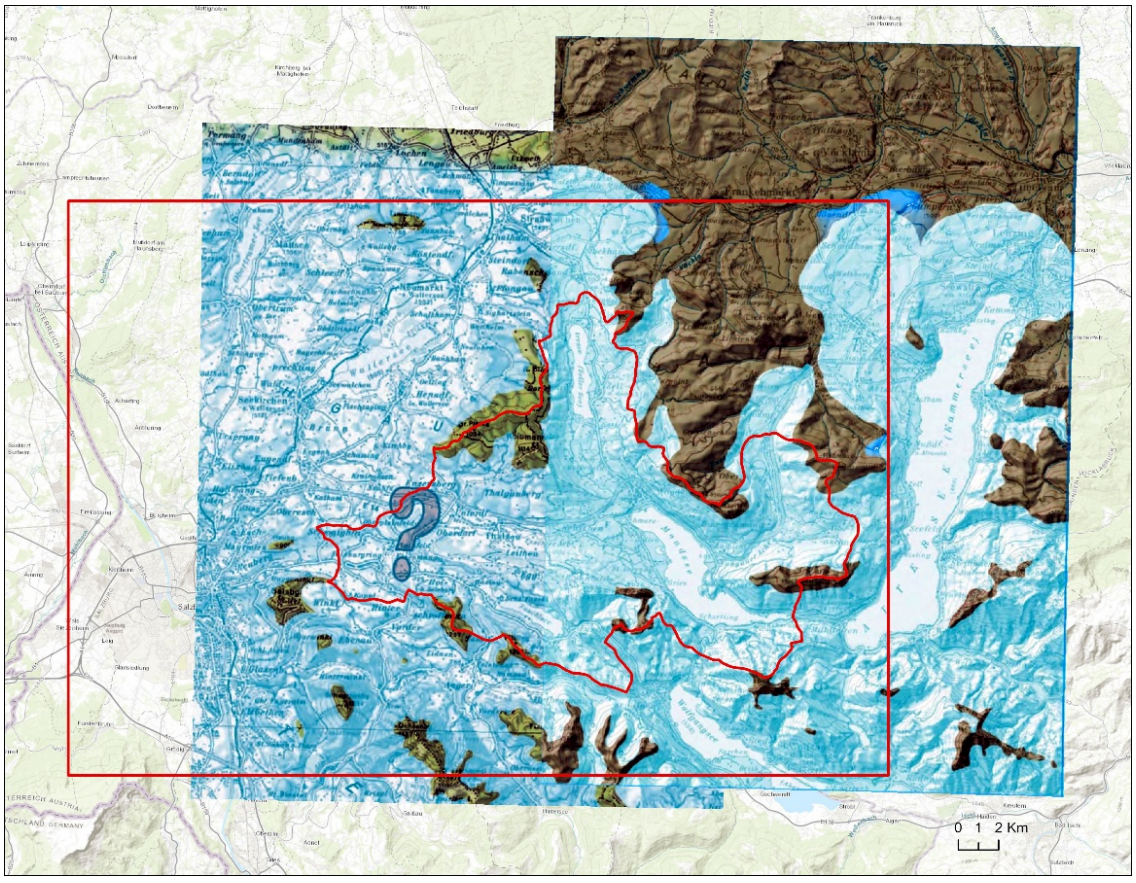

Figure 33: Georectified images showing the Riss glaciation: the left from Egger and Van Husen (2009) and the right from Egger and Van Husen (2014).

Figure 34: Not Georectified image of the Mindel glaciation from Egger and Van Husen (2009).

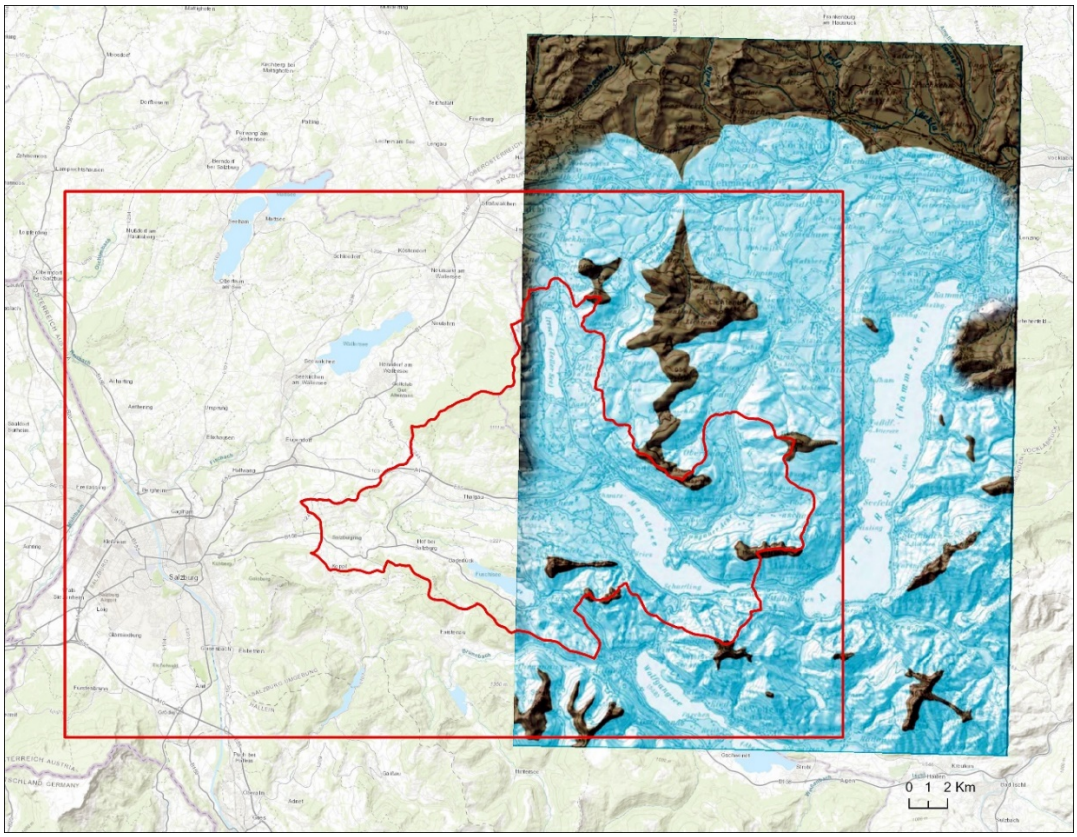

Figure 35: Georectified image of the Mindel glaciation from Egger and Van Husen (2009).

3.3 Interpolation

The points were first interpolated with the Ordinary Kriging method. The Standardized Root Mean Squared Error (RMSE) was near 1, The RMS errors were small, and the Average Standard Error was close to the RMSE. From the interpolated data points a raster layer was deduced with elevation values ranging from ca. 600 m to ca. 1.150 m asl (Figure 36).

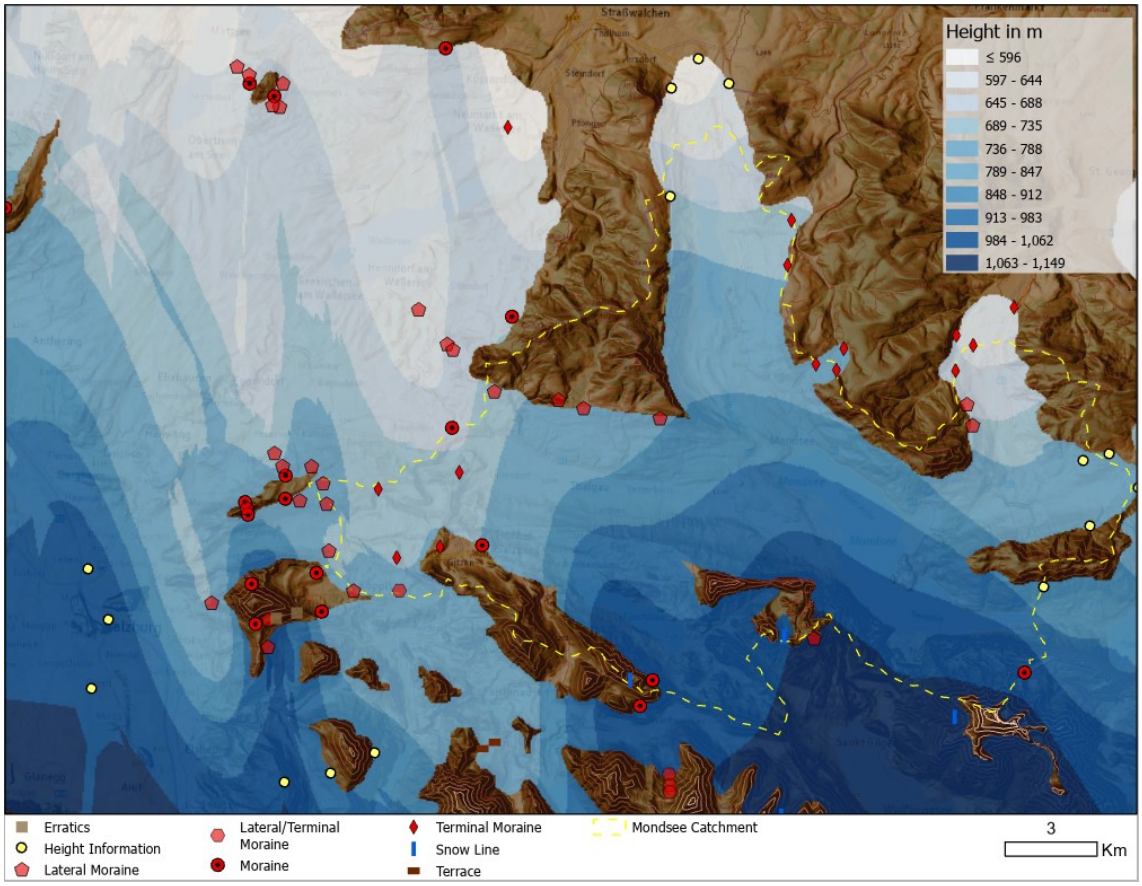

Figure 36: Ordinary Kriging interpolated raster surface of the ice height in the study area and its surroundings.

The same data points were interpolated with the IDW method, and the results were slightly different (Figure 37). Kriging and IDW methods helped visualize the ice masses and the ice height distribution in the area as they were thousands of years ago during the Würm glaciation only by interpolating data points. The Surface Volume tool showed a 90 km^3 volume in the catchment area for the Kriging surface and an 84 km^3 volume for the IDW method.

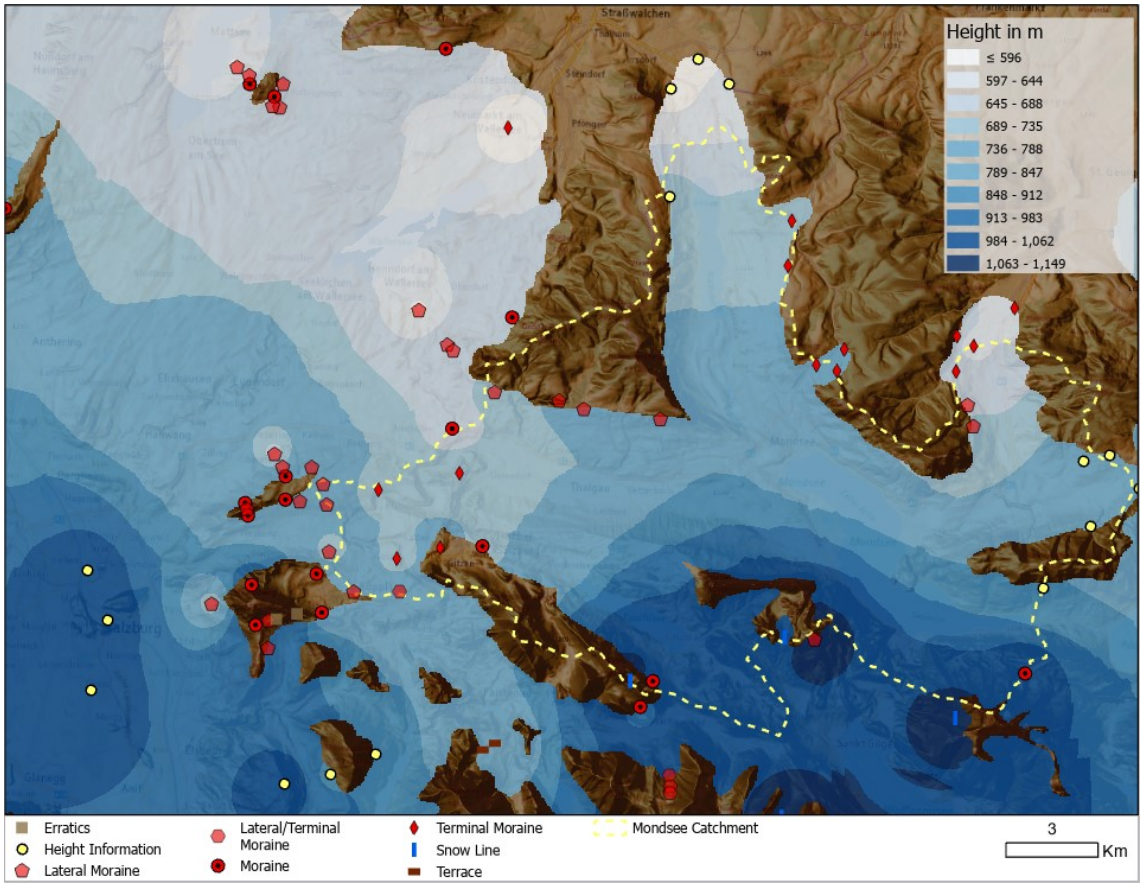

Figure 37: IDW interpolated raster surface of the ice height in the study area and its surroundings.

3.4 Story Map

The results of the study were summarized in a Story Map (Koroxenidou 2022) that can be used while in the field by young scientists or hikers that desire to learn more about the area. Several interactive maps were created showing the origin and present form of lake Mondsee, the ice advance during the four glaciations, but also general information on the area (Figure 38).

Figure 38: Interactive maps created in ArcGIS Online showing from top to bottom: a swipe map of Lake Mondsee and Paleomondsee, a map of the Würm glaciation ice reconstruction, and a map of Lake Mondsee and its catchment, as well as information on the area.

4 Discussion

This study demonstrates the importance of GIS in geomorphologic analysis and its versatility as a tool. With the help of GIS, written information was translated, digitized, and analyzed as points (landform sightings; Table 2), lines (moraines Hochstand and Maximal Stand; chapter 2.1), and polygons (ice masses; chapter 2.1). This procedure was realized by importing JPEG images of the area in a GIS environment and georectifying them. Consequently, the glacial landforms were delineated and presented as a geomorphological map providing further information on the study area and its origins. Lake Mondsee and its "ancestor" Paleomondsee were visualized in 3D and revealed the extent of the lake as it once was and as it is presently. Data points were interpolated, and raster surfaces were created revealing the ice height of the glaciers in the area and were used to calculate the ice volume. Finally, these results, along with the geomorphological map show, that written knowledge can be transferred into the digital world with the help of GIS while at the same time showing that GIS can contribute to a better understanding of the geomorphological structure of an area.

For the **geomorphological analysis**, some classes had high accuracy, and others had low, resulting in a 68% overall accuracy for the OBIA analysis and 45% accuracy for the Pixel-based analysis. Figure 39 shows this difference in accuracy but also the differences between the two methods used. OBIA analysis is more homogenous and gives a better representation of the classification, although there are some obvious misclassifications, for example, the water bodies. In OBIA, the three lakes of the study area are well classified, but some other non-water areas were also classified as water bodies. In Pixel analysis, only Irrsee and Mondsee were classified to some extent as water bodies, whereas lake Fuschlsee was not even included, except for a few pixels.

The unsupervised classification, which is faster but does not take into consideration all the different classes in the image, was also tested. Only four classes were classified with this method and therefore the results were not used for the geomorphological map.

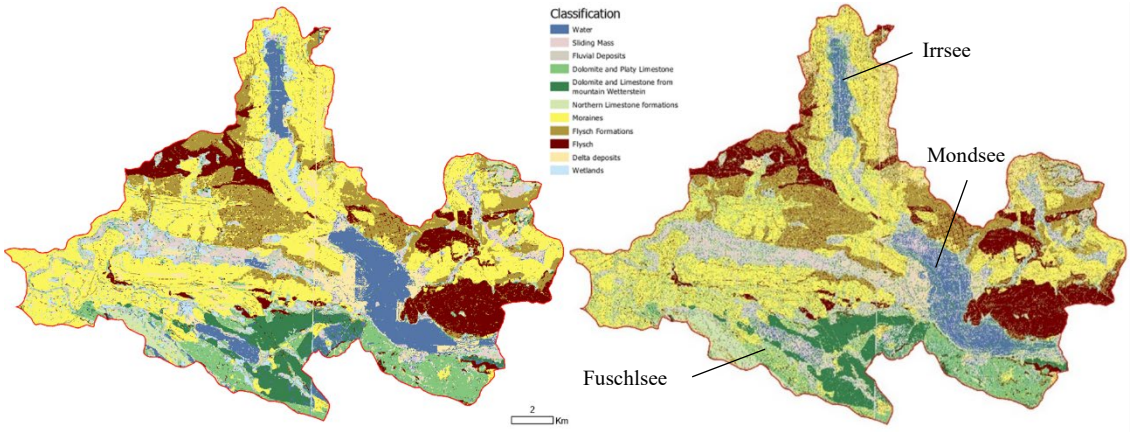

Figure 39: Object-based image analysis (left), and Pixel-based analysis (right).

For the **orthorectification**, higher accuracy with minimum residuals (Root Mean Square, or RMS error) was observed when selecting multiple control points distributed across the images and using the 2nd order Polynomial transformation. Selecting more control points introduced more errors and any attempts to lower the RMS error did not produce good results, but the overall accuracy was increased. The other methods – 1st order Polynomial, Adjust, Projective – were also examined but did not produce as good results as the 2nd order Polynomial, especially along the image's borders.

To evaluate the results of the **orthorectification**, a thorough search by swiping between the layers was conducted throughout the entire image with emphasis on the road intersections, the lake boundaries, and near the edges. The search revealed an overall good adjustment of the images. The issue that arose when the GCPs were distributed evenly across the image and near the edges was that some of the points were selected using the 1-meter base layer and others using the default basemap of the GIS because only a small part of each image was inside the study area, which affected the overall accuracy of the georectification. Another challenge was that the features in the reference base layer and those in the imported images layer were not corresponding since both layers were created in different years. Water bodies, in particular, change over time increasing the errors when selecting GCPs. Another challenge was that some roads which existed in 2009 when the map was created do not exist today because of bypasses constructed in major cities.

After examining the results of the **interpolation**, a "pattern" can be noticed. The ice flows in a direction from south to north following a path from its origin in the Alps towards the foreland with an ice height that is gradually decreasing. The Salzach glacier that passes over the city of Salzburg continues further to the north until Siedelberg (Brückner 1886; Weinberger 1950), west of Mattighofen (Günz glaciation) which is ca. 35 km North of Salzburg. Since Würm was the last glaciation and had less ice accumulation than the other glaciations, it can be said, that the Kriging results predicted the ice coverage to a satisfying degree. The ice height is increased in the south, and as the Traun glacier from the east and the Salzach glacier from the west expand to the north, the height decreases. Although one would expect to see an increased ice height where the Salzach glacier meets the Traun glacier (at Enzersberg, west of Thalgau valley, see also chapter 2.1.1) and above the city of Salzburg and toward the south ice streams should be continuous and not divided into two different height values.

The method of calculating the **ice volume** is not accurate since it involves a raster surface that was predicted from data points which introduced outliers into the analysis and therefore affected the Kriging interpolation as it is sensitive to outliers. Calculating the ice volume is long and laborious work as it involves other crucial information about glaciers, such as the Equilibrium Line Altitude (ELA), flow lines, snow lines, etc. Farinotti et al. (2009) proposed "a method to estimate the ice-thickness distribution and the total ice volume of alpine glaciers from surface topography", however even with this method, "the accuracy inferred from point-to-point comparison of calculated and

measured ice thickness is ~25%". Nonetheless, ArcGIS Pro provided the necessary tools to ensure at least a general picture of how the ice was distributed over the area.

After importing the results of the analysis in a **Story Map**, some limitations were observed, for example, while symbolizing the geomorphological map. The symbolizing options in ArcGIS Pro are wider than those in ArcGIS Online making it easier to symbolize a map digitally as if it was a 2-D map (Figure 29). This function is missing from Online, where it is more practical and less visual. However, on both occasions, the same pop-up appears when clicking on the same polygon (Figure 40). Another limitation of Online concerns visualization on small devices, such as cell phones or tablets. Since these maps were designed to be interactive, it may be impractical to use the story map on a smaller screen such as a cell phone. Although it is functional on a tablet.

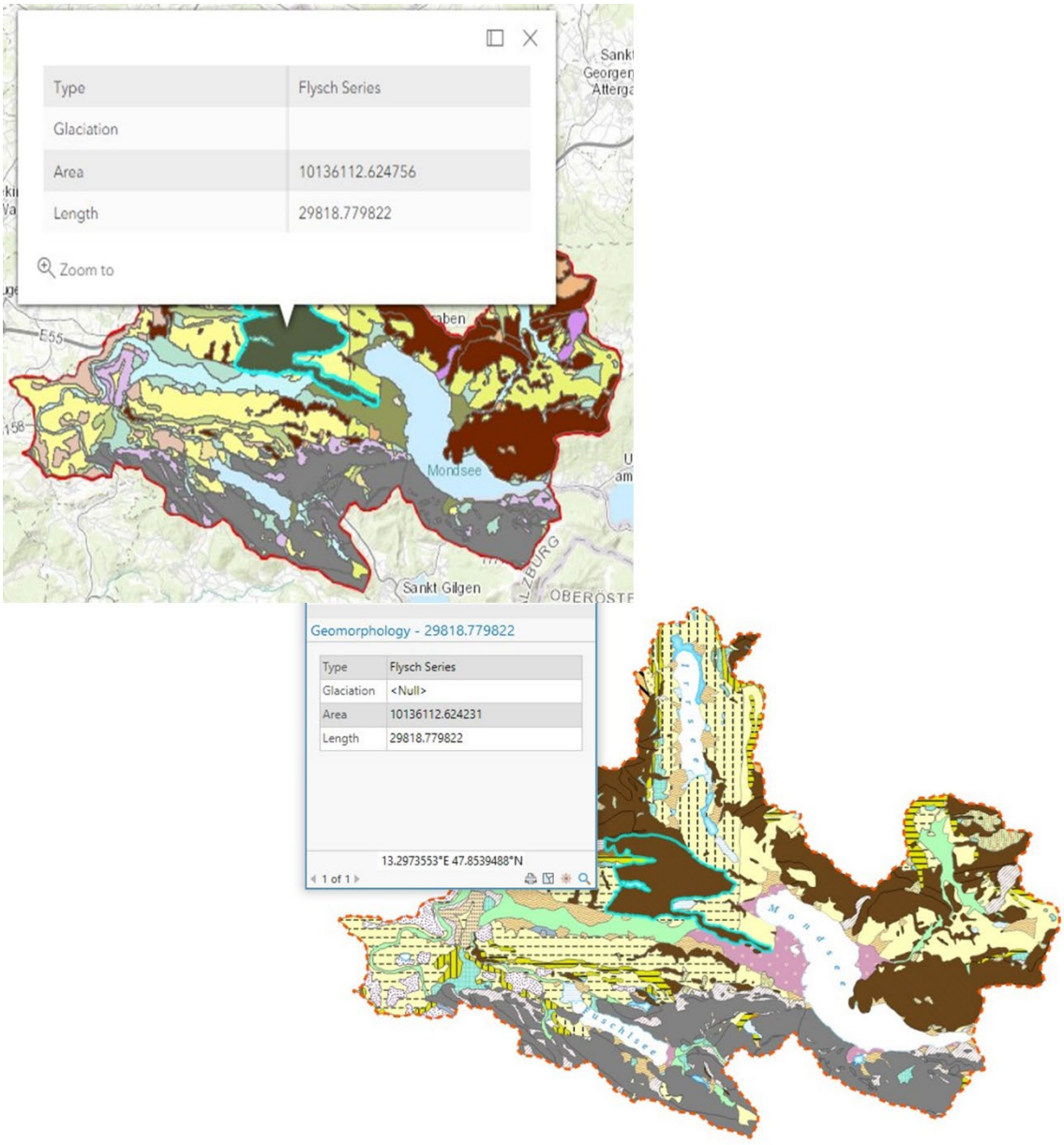

Figure 40: Difference between visualizing a map in ArcGIS Online (top) and ArcGIS Pro (bottom).

Some observations on the data used for the analysis are mentioned below:

According to the report of Van Husen (1986), during the Würm glaciation, the Ackerschneid hill and the hill north of Buchberghütte protruded from the ice as nunataks. But the reconstruction of the glaciation (Figure 41) after Egger and Van Husen (2014) shows these hills covered by ice. For the analysis in this work, the area is considered covered by ice.

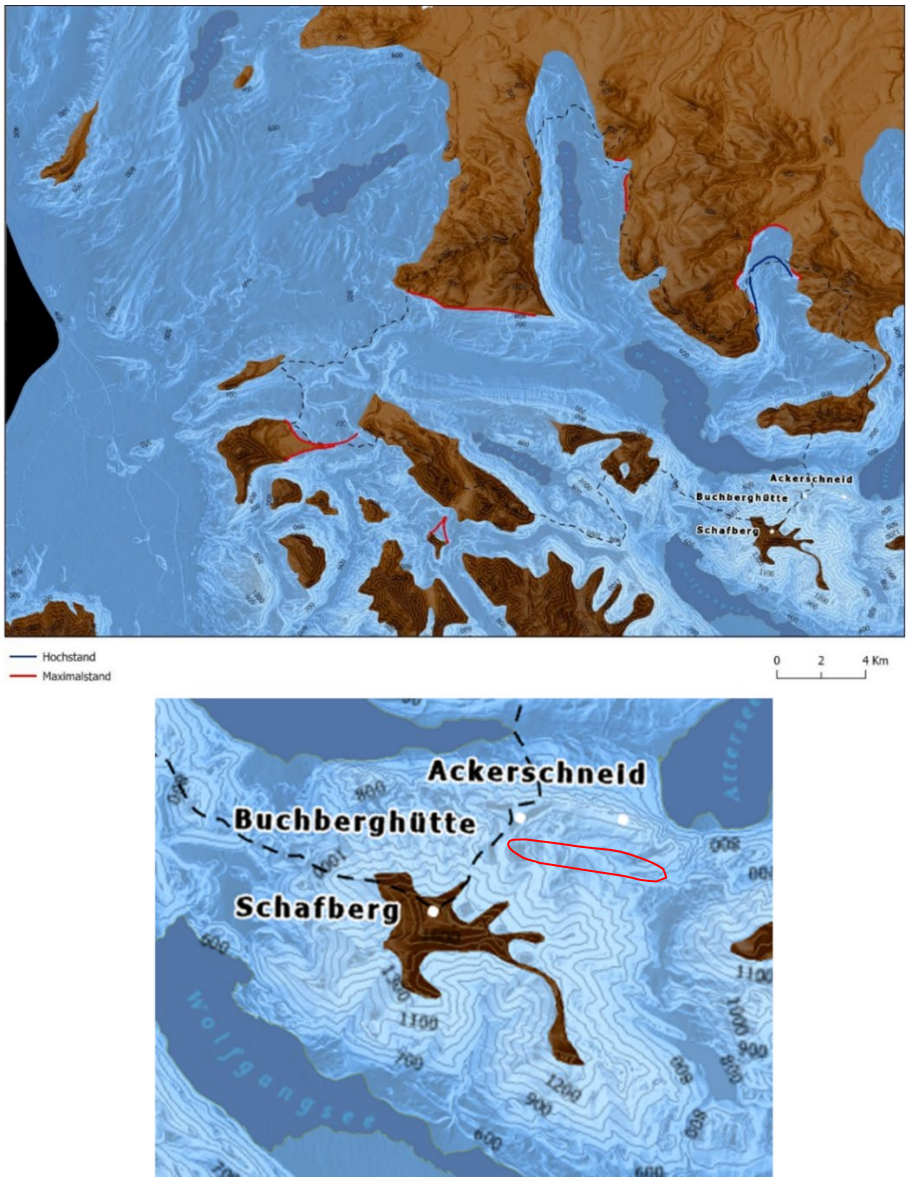

Figure 41: Würm ice reconstruction after Egger and Van Husen (2014).

Moreover, there were some 'inconsistencies' in the data between the reconstruction illustrations regarding the Würm glaciation found in Egger and Van Husen (2009) and Egger and Van Husen (2014). As shown in Figure 42, the nunatak encompassing Schober, Drachenwand, and Plomberg is portrayed differently. In view of the fact that these data were used to reconstruct the ice masses of the glaciation and be used for further analysis

in this work, the model from Egger and Van Husen (2014) was used for the east side of the study area.

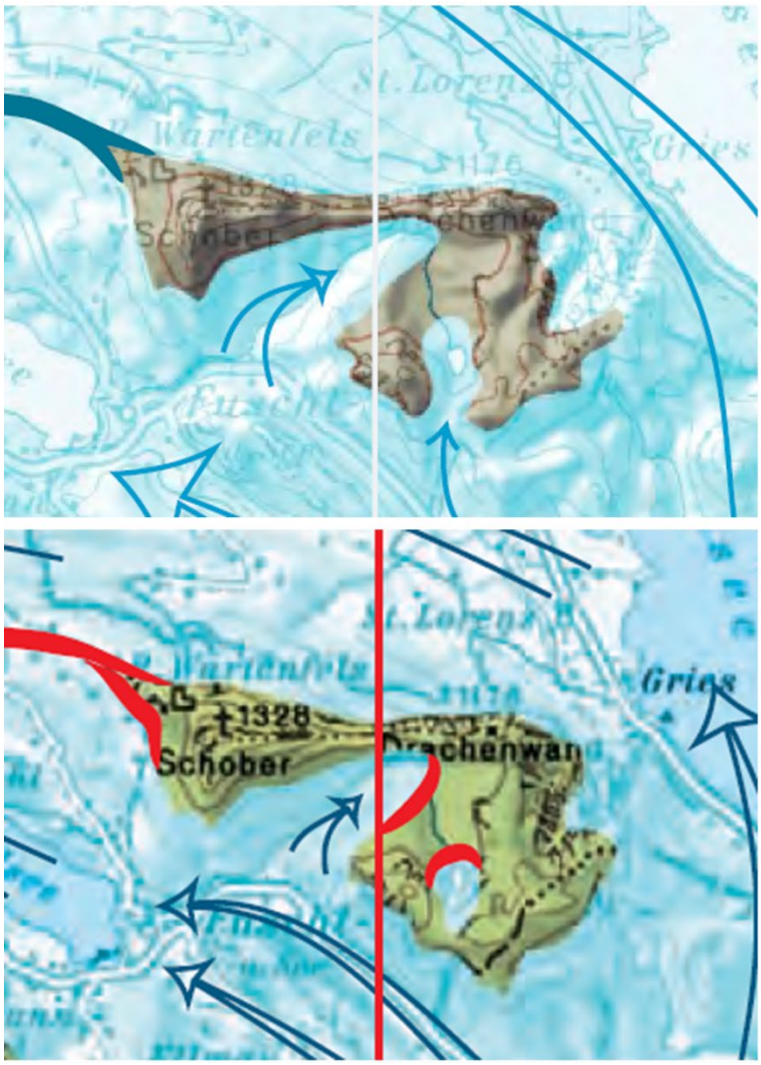

Figure 42: Above Egger and Van Husen (2014) and below Egger and Van Husen (2009).

The same decision was made for another area near Kirchham, where Egger and Van Husen (2009; 2014) presented an area covered by ice in 2009, and in 2014 after further research, the ice coverage was extended. For the analysis in this work, the representation of 2014 was adopted (Figure 43). However, for the mountainous area between lakes Mondsee and Fuschlsee, Schober, the ice reconstruction after Egger and Van Husen (2009) was adopted and not after Egger and Van Husen (2014) since in the latter the reconstruction appears to stop abruptly (Figure 44).

Figure 43: Left picture showing the ice coverage reconstruction of Riss glaciation North of Irrsee lake. The left picture is after Egger and Van Husen (2009) and the right is after Egger and Van Husen (2014). The distinction of the Hochstand and Maximalstand is clear.

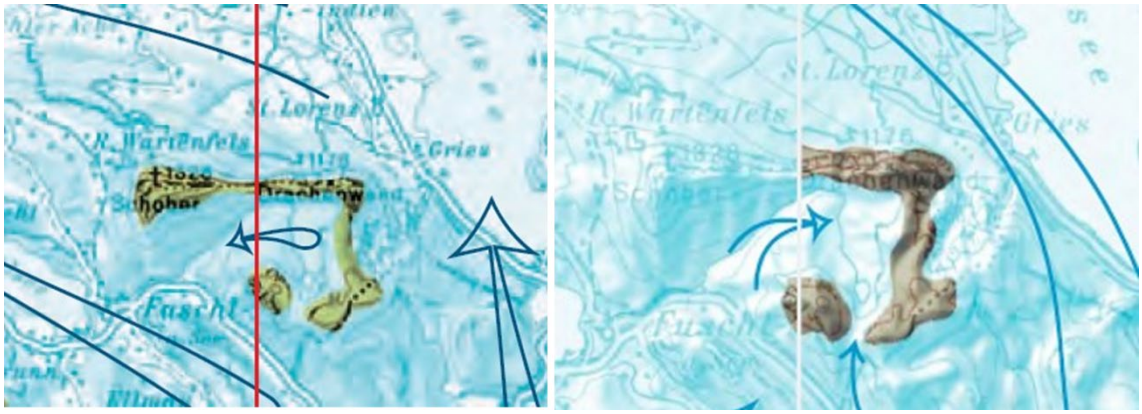

Figure 44: Ice reconstruction of Schober after Egger and Van Husen (2009) (left) and after Egger and Van Husen (2014) (right).

To conclude, the ice reconstruction for the Würm glaciation in Egger and Van Husen (2009) shows the mountain Mühlstein (1059 m height) covered in ice, while for the Riss glaciation, the mountaintop protrudes as a nunatak (Figure 45). Although inconsistent with the fact that the ice during the Würm glaciation was less than that of the Riss and the height of the mountain, this representation was adopted unchanged.

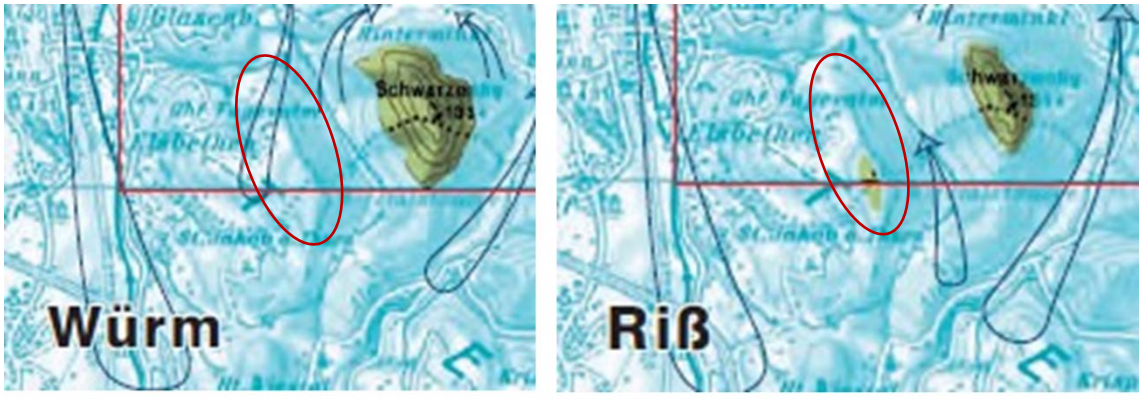

Figure 45: Ice reconstruction of the Würm and Riss Glaciations after Egger and Van Husen (2009).

5 Conclusion and Outlook

Field mapping and the research done by all the experts that were mentioned form the main core of this work, and the means to analyze the geomorphology of an area. However, without GIS it would not have been possible to transfer written knowledge to a computer, analyze the data or even understand the origins of the catchment area, how it was developed, and how its final present form came to be. The background and knowledge of the person conducting the analysis play an important role in the analysis and the way a GIS is being used. In this work, the author has a background in geology but had no prior knowledge of the area, the terrain, or the places that were mentioned. Nonetheless, ESRI's ArcGIS Pro provided all the necessary tools to someone who understands the terrain, and topography of an area through a map and 3D visualization and could conduct a geomorphologic analysis of an area that was previously unknown.

After the first steps of the study were initiated and the first maps were created the author visited parts of the area, namely the Koppl municipality and the regions west of lake Mondsee and also examined the usability of GIS in the field. During this trip, ESRI's application Field Maps was used to view the created maps and recognize some of the glacial landforms also in the field. Other applications such as ArcGIS Earth and Google Earth were used to track the path that was followed with GPS, and geotagged pictures were taken at each stop. Unfortunately, the study was at an early stage and the manually placed points used for the interpolation (Table 2) were not compared with their actual sighting in the field.

In this regard, future work could test the presented points in the field to examine their accuracy, correct them with the exact coordinates of their sighting, and gather more points with the aforementioned applications, thus enhancing the interpolation accuracy and overall analysis. Testing the Story Map in the field could also provide information if the tool is useful or if it still has limitations. Other future work could focus on the extension of the analysis to the other glaciations (Riss, Mindel, and Günz). The ice reconstruction with interpolation and the volume calculation was conducted only for the Würm glaciation. The other glaciations could also be analyzed to calculate the percentage of ice volume loss during each glaciation.

6 References

Aguilar, F.J., Agüera, F., Aguilar, M.A., Carvajal, F., 2005. Effects of terrain morphology, sampling density, and interpolation methods on grid DEM accuracy. Photogrammetric Engineering & Remote Sensing 71, 805–816.

Antoniou, V., Mavroulis, S., Spyrou, N.-I., Bardouli, P., Andreadakis, E., Skourtsos, E., Kaviris, G., Sakkas, V., Carydis, P., Lekkas, E. (Eds.), 2018a. Storytelling Technologies for Dissemination of Scientific Information of Natural Disasters: The June 12, 2017, Mw 6.3 Lesvos (Northeastern Aegean, Greece) earthquake story map. INQUA Focus Group Earthquake Geology and Seismic Hazards.

Antoniou, V., Ragia, L., Nomikou, P., Bardouli, P., Lampridou, D., Ioannou, T., Kalisperakis, I., Stentoumis, C., 2018b. Creating a story map using geographic information systems to explore geomorphology and history of Methana peninsula. ISPRS International Journal of Geo-Information 7, 484.

Baker, T.R., 2015. WebGIS in education, In: Geospatial technologies and geography education in a changing world, Springer, pp. 105–115.

Beiwl, C., Mühlemann, H., 2008. Atlas der natürlichen Seen Österreichs mit einer Fläche≥ 50 ha. Morphometrie-Typisierung-Trophie. Bundesamt für Wasserwirtschaft: Vienna.

Beiwl, C., Rodinger, W., 2010. Natürliche und künstliche Seen Österreichs größer als 50 ha, Bundesamt für Wasserwirtschaft.

Berendsen, M.E., Hamerlinck, J.D., Webster, G.R., 2018. Digital Story Mapping to Advance Educational Atlas Design and Enable Student Engagement. ISPRS International Journal of Geo-Information 7. doi:10.3390/ijgi7030125.

Beven, K.J., Kirkby, M.J., 1979. A physically based, variable contributing area model of basin hydrology/Un modèle à base physique de zone d'appel variable de l'hydrologie du bassin versant. Hydrological Sciences Journal 24, 43–69.

Bishop, M.P., Olsenholler, J.A., Shroder, J.F., Barry, R.G., Raup, B.H., Bush, A.B.G., Copland, L., Dwyer, J.L., Fountain, A.G., Haeberli, W., others, 2004. Global Land Ice Measurements from Space (GLIMS): remote sensing and GIS investigations of the Earth's cryosphere. Geocarto International 19, 57–84.

Blaschke, T., 2010. Object based image analysis for remote sensing. ISPRS Journal of Photogrammetry and Remote Sensing 65, 2–16.

Blaschke, T., Strobl, J., 2001. What's wrong with pixels? Some recent developments interfacing remote sensing and GIS. Zeitschrift für Geoinformationssysteme, 12–17.

Bocco, G., Mendoza, M., Velázquez, A., 2001. Remote sensing and GIS-based regional geomorphological mapping—a tool for land use planning in developing countries. Geomorphology 39, 211–219.

Bolch, T., Kamp, U., 2005. Glacier mapping in high mountains using DEMs, Landsat and ASTER data.

Bonham-Carter, G.F., 2014. Geographic information systems for geoscientists: modelling with GIS, Elsevier.

Boser, B.E., Guyon, I.M., Vapnik, V.N., 1992. A training algorithm for optimal margin classifiers Proceedings of the fifth annual workshop on Computational learning theory, pp. 144–152.

Brown, D.G., Lusch, D.P., Duda, K.A., 1998. Supervised classification of types of glaciated landscapes using digital elevation data. Geomorphology 21, 233–250.

Brückner, E., 1886. Die Vergletscherung des Salzachgebietes: nebst Beobachtungen über die Eiszeit in der Schweiz, Hölzel.

Burnett, C., Blaschke, T., 2003. A multi-scale segmentation/object relationship modelling methodology for landscape analysis. Ecological modelling 168, 233–249.

Campbell, J.B., Wynne, R.H., 2011. Introduction to remote sensing, Guilford Press.

Chaplot, V., Darboux, F., Bourennane, H., Leguédois, S., Silvera, N., Phachomphon, K., 2006. Accuracy of interpolation techniques for the derivation of digital elevation models in relation to landform types and data density. Geomorphology 77, 126–141.

Clark, C.D., 1997. Reconstructing the evolutionary dynamics of former ice sheets using multi-temporal evidence, remote sensing and GIS. Quaternary Science Reviews 16, 1067–1092. doi:10.1016/S0277-3791(97)00037-1.

Darboux, F., Gascuel-Odoux, C., Davy, P., 2002. Effects of surface water storage by soil roughness on overland-flow generation. Earth surface processes and landforms 27, 223–233.

Declercq, F.A.N., 1996. Interpolation methods for scattered sample data: accuracy, spatial patterns, processing time. Cartography and Geographic Information Systems 23, 128–144.

Del Negro, W., 1967. Moderne Forschungen über den Salzachvorlandgletscher. Mitt. der Österr. Geogr. Gesellschaft 109.

Del Negro, W., 1969. Bemerkungen zu den Kartierungen L. Weinbergers im Traungletschergebiet (Attersee-und Traunseebereich). Verhandlungen der Geologischen Bundesanstalt 120, 131–163.

Del-Negro, W., 1957. Bericht über Kartierungsarbeiten in der Gaisberggruppe 1:25.000. Verhandlungen der Geologischen BundesanstaltVerhandlungen der Geologischen Bundesanstalt ; 1957. [in Deutsch].

Demek, J., 1972. Manual of detailed geomorphological mapping, Czechoslovak Academy of Sciences.

Dent, D., Young, A., 1981. Soil survey and land evaluation.

Dikau, R., Brabb, E.E., Mark, R.M., 1991. Landform classification of New Mexico by computer.

Dikau, R., Schmidt, J., 1999. Georeliefklassifikation, In: Angewandte Landschaftsökologie, Springer, pp. 217–244.

Dragut, L., Blaschke, T., 2006. Automated classification of landform elements using object-based image analysis. Geomorphology 81, 330–344.

Draxler, I., 1977. Pollenanalytische Untersuchungen von Mooren zur spät-und postglazialen Vegetationsgeschichte im Einzugsgebiet der Traun. Jahrbuch der Geologische Bundesanstalt 120, 131–163.

Ebers, E., 1955. Hauptwürm, Spätwürm, Frühwürm und die Frage der älteren Würmschotter. E&G Quaternary Science Journal 6, 96–109. doi:10.3285/eg.06.1.10.

Ebers, E., Weinberger, L., Del-Negro, W., 1966. Der pleistozäne Salzachvorlandgletscher, Gesellschaft für Bayerische Landeskunde.

Egger, H., Beiträgen, M., Heinrich, M., Husen, D., Lobitzer, H., Moshammer, B., Pavuza, R., Rupp, C., Schedl, A., Schubert, G., Schuster, R., Stummer, G., Wagner, L., Wessely, G., Abbildungen, Tabelle, 2018. ERLÄUTERUNGEN zu Blatt 67 GRÜNAU im ALMTAL.

Egger, H., Van Husen, D., 2003. Geologische Karte der Republik Österreich 1: 50.000, Blatt 64 Strasswalchen. Geologische Bundesanstalt, https://opac.geologie.ac.at/ais312/dokumente/GK0064_000_A.pdf.

Egger, H., Van Husen, D., 2007. Geologische Karte der Republik Österreich 1:50.000, Blatt 67 Grünau + Erläuterungen.

Egger, H., Van Husen, D., 2009. Erläuterungen zu Blatt 64 Strasswalchen. Geologische Karte der Republik Österreich 1, 50000.

Egger, H., Van Husen, D., 2014. Erläuterungen zu Blatt 65 Mondsee. Geologische Karte der Republik Österreich, 149.

Farinotti, D., Huss, M., Bauder, A., Funk, M., Truffer, M., 2009. A method to estimate the ice volume and ice-thickness distribution of alpine glaciers. Journal of Glaciology 55, 422–430. doi:10.3189/002214309788816759.

Fischer, A., 2009. Calculation of glacier volume from sparse ice-thickness data, applied to Schaufelferner, Austria. Journal of Glaciology 55, 453–460.

French, JR, 2003. Airborne LiDAR in support of geomorphological and hydraulic modelling. Earth Surface Processes and Landforms: The Journal of the British Geomorphological Research Group 28, 321–335.

Frisch, W., 1979. Tectonic progradation and plate tectonic evolution of the Alps. Tectonophysics 60, 121–139. doi:10.1016/0040-1951(79)90155-0.

Froitzheim, N., Schmid, S.M., Frey, M., 1996. Mesozoic paleogeography and the timing of eclogite-facies metamorphism in the Alps: a working hypothesis. Eclogae Geologicae Helvetiae 89, 81.

Fugger, E., Kastner, C., 1885. Naturwissenschaftliche Studien und Beobachtungen aus und über Salzburg., Kerber.

Gamerith, W., Heuberger, H., 1990. Daten zur Eisstromhöhe des eiszeitlichen Salzachgletschers im Salzachquertal zwischen Schwarzach-St.Veit und Salzburg. Gesellschaft für Salzburger Landeskunde.

Gibbard, P., Cohen, K.M., 2008. Global chronostratigraphical correlation table for the last 2.7 million years. Episodes 31, 243–247.

Gold, C.M., 1989. Surface interpolation, spatial adjacency and GIS. Three dimensional applications in geographic information systems 5, 21–35.

Goodchild, M.F., 1993. Data models and data quality: problems and prospects. Environmental modeling with GIS, 94–103.

Goodchild, M.F., Gopal, S., 1989. The accuracy of spatial databases.

Götzinger, G., 1930. Aufnahmsbericht des Chefgeologen Prof. Dr. Gustav Götzinger über Blatt Salzburg (4850). Geologische Bundesanstalt.

Götzinger, G., 1936. Führer für die Quartär-Exkursionen in Österreich, Geologische Bundesanstalt.

Götzinger, G., 1957. Bericht 1956 über Aufnahmen auf Blatt Staßwalchen (64). Verhandlungen der Geologischen BundesanstaltVerhandlungen der Geologischen Bundesanstalt ; 1958. [in Deutsch].

Götzinger, G., 1958. Bericht 1957 über Aufnahmen auf den Blättern Salzburg (63), Straßwalchen (64) mit Vergleichstouren auf den Blättern Ranshofen (45) und Mattighof en (46). Verhandlungen der Geologischen BundesanstaltVerhandlungen der Geologischen Bundesanstalt ; 1958. [in Deutsch].

Graves, M.E., 2015. Spatial narratives of struggle and activism in the Del Amo and Montrose Superfund Cleanups: A community-engaged Web GIS story map, University of Southern California.

Grimm, W.D., Bläsig, H., Doppler, G., Fakhrai, M., Goroncek, K., Hintermaier, G., Just, J., Kiechle, W., Lobinger, W.H., Ludewig, H., others, 1979. Quartärgeologische Untersuchungen im Nordwestteil des Salzach-Vorlandgletschers (Oberbayern). Moraines and Varves, 101–114.

Groshans, G., Mikhailova, E., Post, C., Schlautman, M., Carbajales-Dale, P., Payne, K., 2019. Digital Story Map Learning for STEM Disciplines. Education Sciences 9. doi:10.3390/educsci9020075.

Gustavsson, M., Kolstrup, E., Seijmonsbergen, A.C., 2006. A new symbol-and-GIS based detailed geomorphological mapping system: Renewal of a scientific discipline for understanding landscape development. Geomorphology 77, 90–111.

Harbor, J.M., 1993. Glacial geomorphology: modeling processes and landforms. Geomorphology 7, 129–140. doi:10.1016/0169-555X(93)90014-S.

Hengl, T., Reuter, H.I., 2008. Geomorphometry: concepts, software, applications, Newnes.

Horst Ibetsberger, 2003. Eiszeit und Landschaft. Die Salzach, Wildfluss in der Kulturlandschaft, 20–23.

Hunter, G.J., Caetano, M., Goodchild, M.F., 1995. A methodology for reporting uncertainty in spatial database products. URISA-WASHINGTON DC- 7, 11–21.

Jones, A.F., Brewer, P.A., Johnstone, E., Macklin, M.G., 2007. High-resolution interpretative geomorphological mapping of river valley environments using airborne LiDAR data. Earth Surface Processes and Landforms: The Journal of the British Geomorphological Research Group 32, 1574–1592.

Klaus, W., 1987. Das Mondsee-Profil: R/W-Interglazial und vier Würm-interstadiale in einer geschlossenen Schichtfolge.

Kohl, H., 1958. Unbekannte Altmoränen in der südwestlichen Traun-Enns-Platte. Mitteilungen der Geographische Gesellschaft Wien 100, 131–143.

Kohl, H., 1997. Das Eiszeitalter in Oberösterreich - Abriss einer Quartärgeologie von Oberösterreich. Jahrbuch des OÖ. Musealvereines Gesellschaft für Landeskunde 142.

Kohl, H., 1998. Das Eiszeitalter in Oberösterreich Teil II: Die eiszeitliche Vergletscherung in OÖ. Jahrbuch des OÖ. Musealvereines Gesellschaft für Landeskunde 143, 175–390.

Kohl, H., 2001a. Das Eiszeitalter in Oberösterreich, Teil I. NATURSCHUTZABTEILUNG - OBERÖSTERREICH - GEOLOGIE 23, 18–28.

Kohl, H., 2001b. Das Eiszeitalter in Oberösterreich, Teil II. Natuschutzabteilung - Oberösterreich - Geologie 23/4, 26–35.

Koroxenidou, S., 2022. A Geomorphologic Analysis of the Mondsee Catchment, Story Map, https://storymaps.arcgis.com/stories/0bceed526d114c9e93b11f7ba124c84d.

Lambiel, C., Maillard, B., Kummert, M., Reynard, E., 2016. Geomorphology of the Hérens valley (Swiss Alps). Journal of Maps 12, 160–172.

Land Oberösterreich, 21/08/2021. Land Oberösterreich - Digitales Geländemodell 50 cm (XYZ), https://www.land-oberoesterreich.gv.at/211787.htm, [accessed 21 August 2021].

Land Salzburg, 21/08/2021. Land Salzburg - ALS Befliegungen, https://www.salzburg.gv.at/verwaltung_/Seiten/als_befliegungen.aspx, [accessed 21 August 2021].

Leser, H., Stäblein, G., 1975. Geomorphologische Kartierung: Richtlinien zur Herstellung Geomorphologischer Karten 1: 25 000, Freie Universität Berlin. Institut für physische Geographie.

Leys, K.F., Werritty, A., 1999. River channel planform change: software for historical analysis. Geomorphology 29, 107–120. doi:10.1016/S0169-555X(99)00009-4.

Lichtenecker, N., 1938. Die gegenwartige und die eiszeit liche Schneegrenze in den Ostalpen. Verhandlungsband der III. Internationalen Quartarkonferenz, Wien 1936, 141–147.

Matheron, G., 1960. Krigeage d'un panneau rectangulaire par sa périphérie. Note géostatistique 28.

Matheron, G., 1963. Principles of geostatistics. Economic geology 58, 1246–1266.

McBratney, A.B., Santos, M.M., Minasny, B., 2003. On digital soil mapping. Geoderma 117, 3–52.

Meneweger, H., 1993. Zur Quartären Entwicklung des Gebietes um Koppl - Ebenau - Faistenau, Universität Salzburg, 79pp.

Meschede, M., 2015. Die Entwicklung der Alpen, In: Meschede, M. (Ed.) Geologie Deutschlands: Ein prozessorientierter Ansatz, Springer Berlin Heidelberg, Berlin, Heidelberg, pp. 161–174.

Mitas, L., Mitasova, H., 1999. Spatial interpolation. Geographical information systems: principles, techniques, management and applications 1.

Moore, I.D., Grayson, R.B., Ladson, A.R., 1991. Digital terrain modelling: a review of hydrological, geomorphological, and biological applications. Hydrological processes 5, 3–30.

Otto, J.-C., Prasicek, G., Blöthe, J., Schrott, L., 2018. GIS Applications in Geomorphology, In: Comprehensive Geographic Information Systems, Elsevier, pp. 81–111.

P.V. Arun, 2013. A comparative analysis of different DEM interpolation methods. The Egyptian Journal of Remote Sensing and Space Science 16, 133–139. doi:10.1016/j.ejrs.2013.09.001.

Pain, C.F., 1985. Mapping of landforms from Landsat imagery: an example from eastern New South Wales, Australia. Remote Sensing of environment 17, 55–65.

Patzelt, G., 1980. The Austrian glacier inventory: status and first results.

Penck, A., Brückner, E., 1909. Die Alpen im Eiszeitalter, vol 1-3. Tauchnitz, Leipzig, 393.

Penk, A., Brückner, E., 1902. Die Alpen im Eiszeitalter, 227–231.

Pike, R.J., 2000. Geomorphometry-diversity in quantitative surface analysis. Progress in physical geography 24, 1–20.

Pike, R.J., Evans, I.S., Hengl, T., 2009. Chapter 1 Geomorphometry: A Brief Guide, In: Geomorphometry - Concepts, Software, Applications, Elsevier, pp. 3–30.

Prima, O.D.A., Echigo, A., Yokoyama, R., Yoshida, T., 2006. Supervised landform classification of Northeast Honshu from DEM-derived thematic maps. Geomorphology 78, 373–386.

Quinn, P., Beven, K., Chevallier, P., Planchon, O., 1991. The prediction of hillslope flow paths for distributed hydrological modelling using digital terrain models. Hydrological processes 5, 59–79.

Raymo, M.E., 1997. The timing of major climate terminations. Paleoceanography 12, 577–585. doi:10.1029/97PA01169.

Richter, E., 1888. Die Gletscher der Ostalpen, Engelhorn.

Robinson, A.H., Kimerling, A., others, 1995. Elements of cartography.

Rott, H., 1993. The Austrian Alps. US Geological Survey Professional Paper 1386, 5.

Salcher, B.C., Hinsch, R., Wagreich, M., 2010. High-resolution mapping of glacial landforms in the North Alpine Foreland, Austria. Geomorphology 122, 283–293.

Schaber, P., 2015. Die Reoligotrophierung der Salzburger Vorlandseen Mattsee, Obertrumer See, Grabensee und Wallersee. - in: Land Salzburg (Hg.), Reihe Gewässerschutz 17, 21–72.

Schadler, J., 1958. Zur Geologie der Salzkammergutseen.

Schmid, S.M., Fügenschuh, B., Kissling, E., Schuster, R., 2004. Tectonic map and overall architecture of the Alpine orogen. Eclogae Geologicae Helvetiae 97, 93–117. doi:10.1007/s00015-004-1113-x.

Seefeldner, E., 1961. Salzburg und seine Landschaften.

Sperl, H., 1984. Bericht 1983 über geologische Aufnahmen im Quartär auf Blatt 47 Ried im Innkreis. Jahrbuch der Geologischen Bundesanstalt 127, 209–210.

Tehrany, M.S., Pradhan, B., Jebur, M.N., 2014. Flood susceptibility mapping using a novel ensemble weights-of-evidence and support vector machine models in GIS. Journal of hydrology 512, 332–343.

Tehrany, M.S., Pradhan, B., Mansor, S., Ahmad, N., 2015. Flood susceptibility assessment using GIS-based support vector machine model with different kernel types. Catena 125, 91–101.

Thompson, J.A., Bell, J.C., Butler, C.A., 2001. Digital elevation model resolution: effects on terrain attribute calculation and quantitative soil-landscape modeling. Geoderma 100, 67–89.

Tichy, G., 2000. Die Geologie von Koppl. Eine kleine Gemeinde aber reich an Besonderheiten. Heimat Koppl: Chronik der Gemeinde. Koppl: Eigenverlag der Gemeinde Koppl.

Tobler, W.R., 1970. A computer movie simulating urban growth in the Detroit region. Economic geography 46, 234–240.

Toutin, T., 2002. Impact of terrain slope and aspect on radargrammetric DEM accuracy. ISPRS Journal of Photogrammetry and Remote Sensing 57, 228–240.

Trümpy, R., 1960. Paleotectonic evolution of the Central and Western Alps. GSA Bulletin 71, 843. doi:10.1130/0016-7606(1960)71[843:PEOTCA]2.0.CO;2.

Van Husen, D., 1982. Bericht 1982 über geologische Aufnahmen auf Blatt 64 Straßwalchen.

Van Husen, D., 1983. Bericht 1983 über geologische Aufnahmen auf Blatt 65 Mondsee.

Van Husen, D., 1985. Bericht 1985 über quartärgeologische Aufnahmen auf den Blättern 64 Straßwalchen und 65 Mondsee.

Van Husen, D., 1986. Bericht 1986 über geologische Aufnahmen im Quartär auf Blatt 65 Mondsee.

Van Husen, D., 1987. Die Ostalpen in den Eiszeiten: Populaerwissenschaftliche Veröffentlichungen der Geologischen Bundesanstalt. Vienna, Map, scale 1, 1.

Van Husen, D., 1989a. Bericht 1988 über geologische Aufnahmen auf Blatt 64 Strasswalchen. Jahrbuch der Geologischen Bundesanstalt 132, 546–547.

Van Husen, D., 1989b. Geologische Karte der Republik Österreich 1: 50.000, Blatt 65 Mondsee. https://opac.geologie.ac.at/ais312/dokumente/GK0065_000_A.pdf. Geologische Bundesanstalt.

Van Husen, D., 2000. Geological processes during the Quaternary. Mitteilungen der Österreichischen Geologischen Gesellschaft 92, 135–156.

Van Husen, D., 2003. Als unsere Seen Gletscher waren - Die eiszeitliche Entwicklung im Salzkammergut. Gmundner Geo-Studien.

Van Husen, D., Reitner, J., 2011. An Outline of the Quaternary Stratigraphy of Austria. Quaternary Science Journal 60. doi:10.3285/eg.60.2-3.09.

Weber, D., Englund, E., 1992. Evaluation and comparison of spatial interpolators. Mathematical Geology 24, 381–391.

Weinberger, L., 1950. Gliederung der Altmoränen des Salzachgletschers östlich der Salzach. Zeitschrift für Gletscherkunde und Glazialgeologie 1, 176–186.

Weinberger, L., 1952. Ein Rinnensystem im Gebiete des Salzach-Gletschers. Zeitschrift für Gletscherkunde und Glazialgeologie 2, 58–71.

Weinberger, L., 1955. Exkursion durch das österreichische Salzachgletschergebiet und die Moränengürtel der Irrsee-und Attersee-Zweige des Traungletschers. Verhandlungen der Geologischen Bundesanstalt 1955, 7–34.

Weng, Q., 2006. An evaluation of spatial interpolation accuracy of elevation data, In: Progress in spatial data handling, Springer, pp. 805–824.

Wilson, J.P., Gallant, J.C., 2000. Terrain analysis: principles and applications, John Wiley & Sons.

Zhang, W., Montgomery, D.R., 1994. Digital elevation model grid size, landscape representation, and hydrologic simulations. Water resources research 30, 1019–1028.

Zimmerman, D., Pavlik, C., Ruggles, A., Armstrong, M.P., 1999. An experimental comparison of ordinary and universal kriging and inverse distance weighting. Mathematical Geology 31, 375–390.